State-of-the-art: AI-assisted Surrogate Modeling and Optimization for Microwave Filters

Yang Yu, *Member*, *IEEE*, Zhen Zhang, *Graduate Student Member*, Qingsha S. Cheng, *Senior Member*, *IEEE*, Bo Liu, *Senior Member*, *IEEE*, Yi Wang, *Senior Member*, *IEEE*, Cheng Guo, Terry Tao Ye

***Abstract*—Microwave filters are indispensable passive devices for modern wireless communication systems. Nowadays, electromagnetic (EM) simulation-based design process is a norm for filter designs. Many EM-based design methodologies for microwave filter design have emerged in recent years to achieve efficiency, automation, and customizability. The majority of EM-based design methods exploit low-cost models (i.e., surrogates) in various forms and artificial intelligence techniques assist the surrogate modeling and optimization processes. Focusing on surrogate assisted microwave filters designs, this paper firstly analyzes the characteristic of filter design based on different design objective functions. Then, the state-of-the-art filter design methodologies are reviewed, including surrogate modeling (machine learning) methods and advanced optimization algorithms. Three essential techniques in filter designs are included: 1) Smart data sampling techniques; 2) Advanced surrogate modeling techniques. 3) Advanced optimization methods and frameworks. To achieve success and stability, they have to be tailored or combined together to achieve the specific characteristics of the microwave filters. Finally, new emerging design applications and future trends in filter design are discussed.**

***Index Terms*—AI, computer-aided design, coupling matrix, design knowledge, EM-simulation based design, machine learning, microwave filters, optimization, sampling, surrogate modeling.**

I. Introduction

PASSIVE microwave components and devices are the essential elements (accounted for over 75%) in any microwave circuits and systems [1]. Among them, filtering devices are the most important ones since they have specific functionalities to transmit and attenuate signals operating at specific frequency ranges [2]-[3]. Growing requirements in developing communication technologies, e.g., 5G system and beyond [4]-[5], stimulate advanced emerging fabrication techniques and design theories demanding faster and more accuracy in simulation, modeling, and fabrication of these devices with better performance.

Manuscript received October 9, 2022. This work is partially supported by the National Natural Science Foundation of China Grant 62071211 and also by the UK Engineering and Physical Science Research Council under grant EP/S013113/1 and EP/M013529/1. (Corresponding author: *Zhen Zhang*, *Qingsha S. Cheng*)

Y. Yu is with Key Laboratory of Microwave Remote Sensing, National Space Science Center, Chinese Academy of Sciences, Beijing, 100190, China. (email: issacyu@live.cn)

Z. Zhang is with School of Electronics and Communication Engineering, Guangzhou University. (email: zhangzhen@gzhu.edu.cn)

Q. S. Cheng and Terry Tao Ye are with the Dept. of Electrical and Electronic Engineering, Southern University of Science and Technology, Shenzhen, 518055, China. (emails: chengqs@sustech.edu.cn, yet@sustech.edu).

Y. Yu and Y. Wang are with the School of Electrical, Electronic and System Engineering, University of Birmingham, Birmingham B15 2TT, U.K. (e-mail: y.wang.1@bham.ac.uk).

B. Liu is with James Watt School of Engineering, University of Glasgow, Glasgow, Scotland. G12 8QQ, U.K. (e-mail: bo.liu@glasgow.ac.uk).

C. Guo is with Dept. of Information and Communication Engineering, Xi'an Jiaotong University, Xi'an, CN 710100, China (email: guocheng@xjtu.edu.cn).

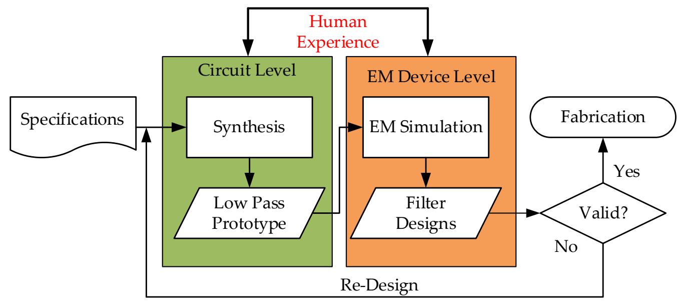

Fig. 1. A general traditional design flow for microwave filters.

Rapid developments of electronic design automation (EDA) software and computing power over the past decades make microwave filter designs much easier than ever before [6]. Both efficient equivalent circuit-based simulation and accurate full-wave electromagnetic (EM) simulation can be implemented [7]. Especially, the EM simulation results are almost the same as the fabricated ones nowadays. These commercial software tools enable more diverse and complicated filter designs customizing various manufacturing techniques with inherent constraints. Note that the EM simulation cost is usually related to the complexity of the filter design [7]. The simulation time might range from several minutes, hours, or even being prohibited for the most complicated and electrical large full-wave design problem, e.g., a multiplexer with a dozen channel filters.

According to the application requirements and circumstances, filter design requires multiple steps with several concerns, e.g., loss, bandwidth, operating frequency, stopband rejection, wideband performance, physical size, weight, operating power, stability, etc. [2]. Fabrication techniques and basic transmission elements have to be first determined before to the formal design process [8]. With essential electrical parameters of design material and fabrication constraints, designers investigate the basic principle of the microwave elements and their coupling structures using the essential electrical parameters of design material and fabrication constraints. EM simulation-based parameter sweeping, or scaling is manipulated with designers to learn basic EM trends of resonator modes and coupling structures. Traditionally, the

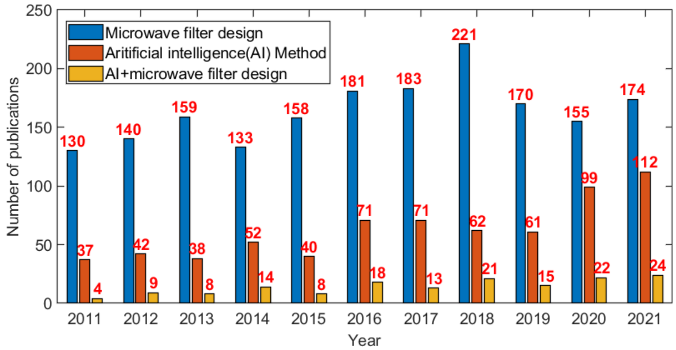

Fig. 2. Statistics of the number of publications in IEEE Microwave and Wireless Components Letters and IEEE Transactions on Microwave Theory and Techniques related to the “Microwave filter design”, “Artificial intelligence method” and “AI + microwave filter design”.

filter is designed in the process shown in Fig. 1. In this process, the filter specifications are converted into concrete goals which are realized by a designer supervised process. Two most important steps are implemented: synthesis and EM-simulation-based design/optimization.

The synthesis works at the circuit level for accessing a suitable filter topology is based on the design specifications and corresponding element values of the theoretical low-pass prototype [2]-[3], e.g., equivalent circuit or coupling matrix. Therefore, it usually serves as “knowledge” for all following filter designs. In the next stage, designers then tune and scale the physical EM-simulation models using the “knowledge” gained via synthesis. Designers have to make efforts to ensure that the filter’s EM performance matches with the “knowledge” (synthesis results).

Conventionally, there have been several analytical EM design methods for filters [9]-[12]. They are, however, only suitable for a limited number of filters with specific structures or junctions [13]. To be more general, EM simulation-based simulation is required which causes the electrical performance of the microwave filters to achieve a desired performance by altering design parameters. Iterative optimization is frequently used in the EM simulation-based design process. This step converts the design specifications into appropriate objective functions and employs specified optimization methods to find filter designs that fulfill the optimization goals. An iterative brute-force optimization is often prohibitive, especially when the filter structure grows more complicated, e.g., higher-order, cross-couplings, multiple bands, and multiple channels (diplexers and multiplexers). On the other hand, the computer is not yet smart and user-friendly enough to liberate designers from supervision and intervention. In fact, more often than not, designers have to “teach computers” (e.g., manually adjusting) step by step to realize their design goals. Typically, this is a time-consuming, unreliable, or even unsuccessful procedure.

Automation of filter design has long been explored in order to enhance the design efficiency, customizability and reduce the human interaction [2]. A rising number of computational intelligence approaches also known as artificial intelligent (AI) method are incorporated in the filter design process in recent years. Recent decade publications related to the topics of “Microwave filter design”, AI method including “machine

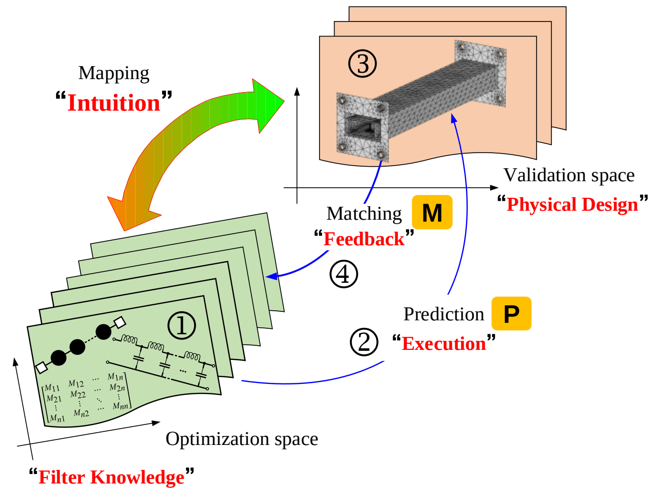

Fig. 3. The design process of filters based on space mapping (SM). Matching (“M”) and prediction (“P”) are usually employed with AI techniques, and they belong to a surrogate-assisted optimization framework.

learning”, “neural network”, “Gaussian process”, “support vector machine”, “heuristic optimization”, etc.” and “AI + Microwave filter design” in IEEE Microwave and Wireless Components Letters and IEEE Transactions on Microwave Theory and Techniques are counted and compared using the “IEEE explore” as shown in Fig. 2. It is worth noting that the topic of “Microwave filter design” has remained heated over recent years. The topic of AI has recently received a great deal of attention, especially in the last five years, and the number of papers has started to rise dramatically. “AI + filter” accounts for a small portion of all articles, but it has a great increasing trend. When compared to “microwave filter design”, the number of publications on “AI + filter” has increased by roughly 10%.

Microwave filter design automation have been investigated around for a long time [14]. It was referred to as a computer-aided design (CAD) technique. The space mapping (SM) technique [15] is likely the most prevalent one for those components. Rather than direct optimization of the filter EM models, many evaluations of a coarse model with low-fidelity and a few evaluations of a fine model with high-fidelity are employed in the SM methods [15]. Drawing on the overall notion of SM [16], Fig. 3 depicts a filter design process employing SM's coarse and fine models. Computationally efficient coarse models, such as equivalent circuits, are not very accurate, whereas computationally expensive fine models, such as full-wave EM simulation models, are sufficiently accurate. The same design parameters in two models should exhibit different but correlated behaviors, indicating that the design parameters play two correlated roles in two spaces. A relationship or discrepancy can be discovered between two spaces through “Matching (M)” and “Prediction (P)”. The coarse model is then combined with the discrepancy to produce a surrogate. “P” generates the design candidate and send it to the fine model for validation, if the design specification is unsatisfied, the design parameters are sent back (“M”) to the coarse model for further optimization. Following an iterative optimization of the coarse model, the surrogate is updated. The mapping elements (“intuition”) that align the coarse model as a surrogate model of the fine model are denoted by the difference between the coarse and fine models. When satisfied accuracy can be achieved, the surrogate will combine the fine model's accuracy with the coarse model's efficiency. Many advanced SM concepts have been proposed, e.g., aggressive SM [17], implicit SM [18], neural SM [19]-[21], cognition-driven SM [22]-[25], and tuning SM [26]-[33], etc. Impressive examples include a 10-channel dielectric multiplexer [34] with up to 140 variables and a SIW multiplexer [35] with 63 variables that have been successfully designed based on aggressive SM.

Most surrogate assisted filter design techniques have so far been built on the concept of SM techniques [36], in which "M" and "P" processes are frequently used. They are known as a surrogate-assisted optimization (SAO) framework [36] and are distinguished from direct EM optimization on the fine model [37]-[38]. Physical SAO and data-driven SAO approaches are two types of SAO. Clearly, the original SM approaches are part of a normal physical SAO method, in which the surrogate is modeled using the natural coarse (theoretical) filtering models, e.g., equivalent circuits or coupling matrices [2]-[3]. In some circumstances, the prediction from the physical models has a lower correlation with the fine model. Note that the theoretical models can only represent the basic theoretical filtering responses based on the design specification rather than describing all the practical filter behaviors [6], e.g., dispersion, radiation, power handling, thermal stability, losses, parasitic coupling, spurious wideband performance, etc. This attributes that obtaining a high-quality surrogate model is difficult. The data-driven SAO approaches, on the other hand, learned the filter EM characteristics using a data set derived from simulation or measurement data. Machine learning techniques are frequently used in the data-driven SAO. They can effectively model fine models' nonlinear EM behavior. Therefore, the data-driven SAO techniques with more generality have become more popular in recent years. This work is mostly concerned with them.

In recent years, a growing number of unique and advanced AI-assisted surrogate modeling and optimization methods are developed for filter designs, but seldom of them can systematically explain why these methods are effective. To solve this problem, the problem characteristics of filter design are investigated in this paper. Characteristics landscapes of four different objective functions are investigated on the basis of parameter sampling on a directly coupled resonator filter. This also benefits for selection of suitable SAO framework for a given challenging problem. Then, some advanced EM optimization methods with selected applications in microwave filter designs are reviewed in the aspects of smart sampling methods, advanced surrogate modeling methods, and effective optimization algorithms and frameworks, respectively. Finally, future expectations are explored based on the emerging important applications.

The organization of this paper is as follows. Section II overviews the design flow for microwave filters and investigates their characteristics using a case study. Section III reviews the state-of-the-art AI assisted surrogate modeling and optimization approaches for microwave filter design problems with the selected applications. Section IV discusses some emerging techniques for designing microwave filters and outlooks on the future research. Section V concludes this paper and reinforces the important aspect of SAO techniques playing in microwave filter design.

II. An Overview of Microwave Filter Design

A. *Filter design process*

It is usually not straightforward to design a usable filter from a design specification [2]-[3]. Synthesis, physical dimensioning and EM optimization are the most important processes in a typical microwave filters design routine. Fig. 4 illustrates the detailed procedures incorporated with different of automation levels (Section II(B)) for them. The filter design processes are briefly introduced in the following:

Synthesis. This step aims to generate theoretical element values for a specific topology related to the filter design specifications, i.e., a coupling matrix or equivalent circuit [2]. To begin with, the filtering specifications are transferred to the normalized frequency ranges. According to the preassigned requirements, ideal filtering responses are represented by using mathematical polynomials in the normalized frequency range [2]. Then, a filter topology is chosen for synthesis where the relationship between low-pass prototype elements and theoretical filter responses are constructed. Analytical methods have been employed to obtain the element values for specific topologies [39]-[40]. To be more general, optimization-based synthesis methods is employed for most topologies, especially when analytical synthesis is unattainable [41]-[42]. The optimization-based synthesis is more straightforward as the polynomial synthesis can be omitted since there is a direct relationship between the low-pass prototype and filter responses. The "distance (error function)" between them can be calculated. When the error function is minimized through local or global optimization, the desired low-pass prototype can be achieved. Examples includes gradient-based local optimization method [41], global optimization method [42]-[43], and memetic optimization method [44]. The synthesis result (filter topology and coupling matrix) is used as the "knowledge" to guide the subsequent design process at this point.

Electromagnetic (EM) element design and physical dimensioning. The obtained synthesis results are denormalized into the real frequency range and element values are converted into physical structures in this step. Based on the EM behavior of the selected resonators and coupling structure, the operation ranges and configurations of the filter are built. Then, the physical initial dimensions for each element are predicted, including resonator dimensions and coupling structures dimensions [2]-[3].

The most widely used method is the curve fitting method [2]-[3]. Two design curves describe the mutual couplings between resonator pairs and the external quality factor between the resonator and I/O ports. The mutual coupling values and external quality factor values are calculated from either frequency-domain simulation or eigenmode simulation results by sweeping the dimension parameters with discrete samples.

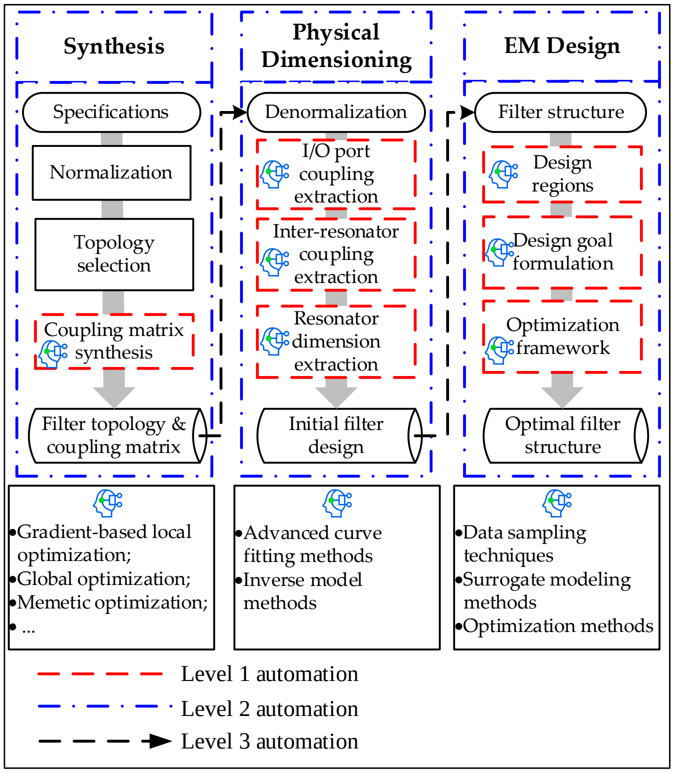

Fig. 4. The main filter design process.

When changing parameters, the center frequency of the simulation results must be held at a specific frequency point, i.e., the center frequency of the filter. Then, the curves are fitted as a function to produce the geometrical dimensions corresponding to expected coupling values. However, experience-based estimation is often required in the original method [2]-[3], e.g., order of fitting curve and number of samples. When it comes to the filter with complex structures (e.g., cross-couplings and junctions), this method will become inaccurate.

To increase the accuracy, some research studies used more complex curve fitting techniques or modeling methods to develop an inverse model, such as quadratic polynomials [45], sparse grid interpolation [46], multi-valued polynomials [47]-[48], and artificial neural network [49]. The relationships between each coupling value and multiple adjacent dimensions are learned by this model where the input is a set of coupling coefficients, and the output is the dimensions corresponding to the set of coupling coefficients. The ensuing problem is that more EM simulations are required for complex curve fitting and modeling. As the initial design is predicted based on the theoretical values, the extracted filter dimensions usually do not satisfy the design specifications, but only can they provide a good initial design for the final optimization [2], [6].

3-D EM optimization. The filter is finally realized in this step. The obtained initial dimensions are optimized or refined to satisfy the specified requirements guided by synthesis results. This is more complex than the first two procedures. In this process, the optimization region, design objective function, and also optimization methods work together to obtain the optimal results. In recent years, SAO approaches are used to automate the entire procedure and accelerate the optimization assisted by using AI techniques. Smart sampling, advanced surrogate modeling and effective optimization should be concerned and they should be carefully adjusted based on the characteristics of the filter design problems.

B. Automation levels of the microwave filter design

As shown in Fig. 4, there can be three levels of automation in filter design, where the different levels are marked out using different line styles. Also, some of the computational intelligent (i.e., AI) methods that have been used are listed in the bottom and marked out with a blue AI logo. The different levels are explained in the following.

- Level 1 automation: *Designer supervised design*. They are marked out using red dash lines. It can be noticed that one or some steps can be realized by using simple AI techniques, but links between them, realizing direction and decisions are mainly determined by designer interaction.
- Level 2 automation: *Partial automated design*. They are denoted by blue dot-dash lines. This level is mainly focused by current research works. Key intermediates are obtained partially automated using advanced AI techniques, e.g., optimal design employing surrogate assisted EM design methods. Human experience and design knowledge are frequently incorporated into these procedures to automate the links between level 1 automation blocks. However, the methods can be ad-hoc since settings in utilized algorithm necessitate human judgement based on the problem characteristics. Due to different tools utilized, the data transfer, conversion and modeling have to be realized by designers, which are hard to be finished automated without human interactions. For example, the 3D filter model has to be design and modeled by designers before of the initial design assignment.
- Level 3 automation: *Fully automated design*. It is denoted by the black dash line with an arrow. This can be seen as an ultimate goal for our filter design automation. Optimal filter design can be automated derived from specification using AI techniques without human intervention.

This paper mainly focuses on the 3-D EM optimization for microwave filter design with level 2 automation, where AI-assisted surrogate modeling and optimization are mainly applied. In the following two subsections, the “knowledge” in filter design and the characteristics of microwave filter design are investigated. Then, the popular SAO techniques in filter design are reviewed and discussed in Section III.

C. “Knowledge” in the filter design

As previously stated, the synthesis results including the equivalent circuit and coupling matrix, serve as “knowledge” for optimization. The equivalent circuit and coupling matrix are used as surrogates in SM framework to begin with. Moreover, they also create initial designs for the EM simulation-based optimization. Further, the synthesized ideal filtering responses can be also employed as optimization “knowledge” goals (objective function).

The microwave filter is a typical two-port network. The most

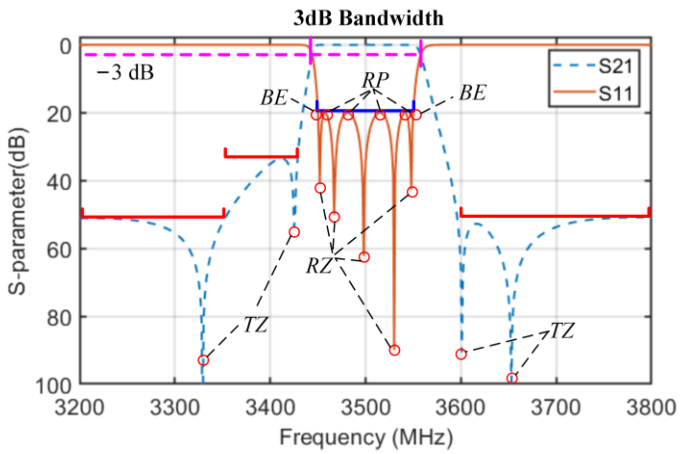

Fig. 5. The critical performance and features in a filter with Chebyshev responses.

TABLE I

THE KNOWLEDGE AND ITS FUNCTIONS IN EM OPTIMIZATION

Knowledge	Functions in EM optimization
Equivalent circuit	Provide initial design, surrogate
Coupling matrix	Provide initial design, surrogate
Synthesized S-parameter responses	Construct the objective function
The magnitude of the S-parameters	Construct the objective function
Feature zeros and poles of S-parameters	Construct the objective function
Coarse mesh model and its derivatives	Surrogate

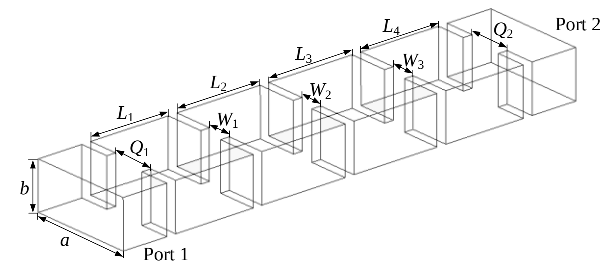

Fig. 6. A 4th order waveguide filter. L_1, …, L_4 are the lengths of the resonators. W_1, …, W_3 are the iris widths of inter-resonator couplings. Q_1 and Q_2 are the iris widths of the external port couplings. The thickness of all the irises is equal to 2 mm.

important description for those passive devices is the S-parameters performance in dB which are normally adopted and formulated in the optimization objective function [2]-[3]. Take a practical case study to illustrate the "knowledge" in the filter responses. A design specification requires the passband operates at 3450 - 3550 MHz and the stopband rejection are $S_{21} < -50$ dB (3200 - 3350 MHz), $S_{21} < -30$dB (3350 - 3420 MHz) and $S_{21} < -50$ dB (3600 – 3800 MHz). The design specifications are straightforward knowledge that can be formulated as magnitude values in objective function guiding the optimization.

To synthesis a filter with Chebyshev responses satisfying the design specification, the specifications are first normalized into a low-pass band [13]. Then, four transmission zeros are assigned at $-j3.5$, $-j1.5$, $j2$, and $j3$. The transmission zeros can suppress the stopband rejection but also sharpen the two roll-offs of S_{21} in the stopbands. The optimal filter polynomial can be obtained [2] as shown in Fig. 5. This is the target of the low-pass prototype synthesis and physical realization of the filter. Besides the magnitude of the S-parameter responses, some important feature frequency points in the filtering responses can also be considered, including reflection zeros (*RZ*s), reflection poles (*RP*s), band edges (*BE*s), and transmission zeros (*TZ*s) [38]. For the detuned filter (un-optimal) responses, the passband bandwidth is hard to be extracted. 3-dB bandwidth is an alternative bandwidth indicator to characterize the filter.

As said that an equivalent circuit is difficult to obtain, EM simulation models using coarse mesh and their responses' derivatives to the design parameters are employed as the "knowledge" to construct surrogate [50]. This is because the less-accurate coarse mesh EM model is computationally faster than the fine mesh EM model, but it maintains high-correlation to the fine EM model's behavior.

All the above-mentioned knowledge and their functions in the EM optimization are summarized as shown in Table 1.

D. Characteristics of microwave filter design

The challenges of microwave filters mainly come from the characteristics of the design landscape represented by the objective function varying with respect to the design parameters [51]. It is worth investigating the characteristics of different forms of the objective function, which benefits appropriate implementing optimization. As discussed, the objective function for microwave filters always employs S-parameter responses with different manipulations in one or several specific frequency ranges and it is minimized in optimization. A fourth-order direct-coupled waveguide filter is taken as an example in the investigation as shown in Fig. 6. The filter contains 9 variables: $\boldsymbol{x} = [W_1, \ldots, W_3, L_1, \ldots, L_4, Q_1, Q_2]$ (mm) which are mutual coupling irises, resonator lengths and I/O port couplings. The passband of the filter is operating at 9.95-10.05GHz and return loss is 20 dB. The optimal design values for this design specification are: W_1 = 5.35217, W_2 = 4.96432, W_3 = 5.35217, L_1 = 17.7731, L_2 = 19.0648, L_3 = 19.0648, L_4 = 17.7731, Q_1 = 9.46258, Q_2 = 9.46258 (mm). The optimal simulated S-parameter responses are shown in Fig. 7(a). The characteristic landscapes based on different objective functions are investigated based on parameter sweeping. The parameter for this filter can be divided into two categories: couplings parameters (coupling iris widths) and resonance parameters (resonator lengths). Three pairs of parameters are selected and combined in parameter sweeping, respectively, as listed in Table II. The dimensions are evenly sampled in the corresponding ranges. There are 900 samples in each combination. The S-parameter variations for each combination are shown in Fig. 7(b)-(d). It can be noticed that 1) Variation W_1 and W_2 have more effect on the magnitude of return loss and less effect on the frequency shift. 2) Variation L_1 and L_2 have more effect on the frequency shift. As the frequency shift, the return loss performance is correspondingly getting worse. 3) Variation W_1 and L_1 have an effect on the center frequency and magnitude of return loss.

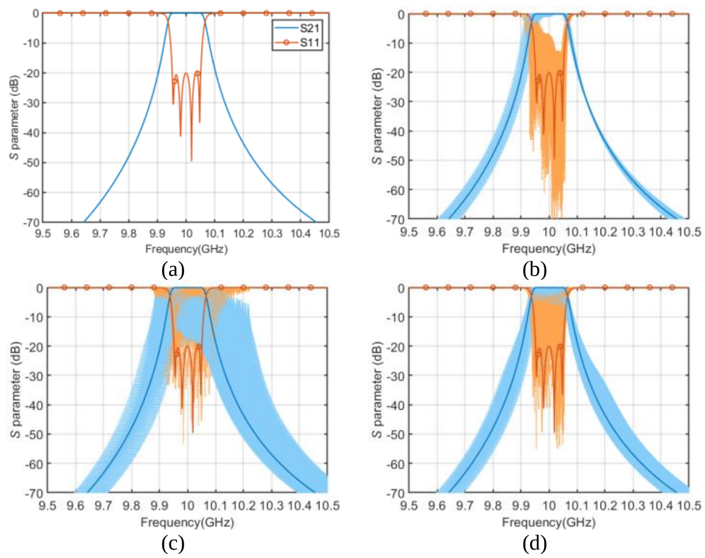

Fig. 7. Simulated S-parameter responses compared with the optimal S-parameter responses (a) based on the parameter sweeping with (b)-(d) the three sweeping combinations.

TABLE II
PARAMETER SWEEP PLAN FOR THE 4TH ORDER BANDPASS WAVEGUIDE FILTER

x_1	x_2	Sampling number
$5.1<W_1<5.6$	$4.7<W_2<5.2$	30×30
$17.2<L_1<18.2$	$18.4<L_2<19.4$	30×30
$5.1<W_1<5.6$	$17.2<L_1<18.2$	30×30

Four different types of widely used objective functions are investigated. To simplify the investigation, only the return loss performance (S_{11}) is considered. They are respectively introduced in the following.

1) Maximum S_{11} within the passband:

$$F_1 : \text{Minimize}\left\{\max\left(\max S_{11.\text{dB}}\left(PB\right)-\left(-20\right),0\right)\right\} \quad (1)$$

where max$S_{11.\text{dB}}$ means the maximum magnitude of S_{11} in dB. PB = (9.95, 10.05) denotes the passband range. This objective function is mostly used in the filter design. When the maximum value of S_{11} within 9.95-10.05 is lower than −20, the F_1 will be zero.

2) Sum of S_{11} magnitude values at sampled frequencies within the passbands:

$$F_2 : \text{Minimize}\left\{\sqrt{\sum_{i=1}^{N}\left(\max\left(S_{11.\text{dB}}\left(f_i\right)-\left(-20\right),0\right)\right)^2}\right\} \quad (2)$$

where N is the number of sampled frequency points, $f_i \in$ (9.95, 10.05) is the sampled frequency point. This objective function aims to evenly minimize the magnitude of the return loss within the passband. To decrease the computational burden, the response within the passband is uniformly sampled. N = 50 for this example. When the sampled S_{11} values are lower than −20, F_2 will be zero.

3) The magnitude of poles of the S_{11}:

$$F_3 : \text{Minimize}\left\{\sum_{i=1}^{N_{RP}}\left(S_{11.\text{dB}}\left(RP_i\right)-\left(-20\right)\right) + \sum_{j=1}^{2}\left(S_{11.\text{dB}}\left(BE_j\right)-\left(-20\right)\right)\right\} \quad (3)$$

where RP_i is the ith theoretical reflection poles of S_{11} within the passband. N_{RP} denotes the number of the RP. The desired poles for this filter example are 9.9646, 10.0353 and 10. (GHz). BE_i denotes the ith band-edge of the desired S_{11}. 9.95, and 10.05 are band-edges in this example. This objective function is another type of objective function based on sampled S_{11}, but the selected frequencies are key features in desired S_{11} response.

4) Feature-assisted objective function: This objective function is proposed in cognition-driven space mapping technique [22]-[25]. The objective function is formulated with the assistance of the reflection zeros in the candidate responses during optimization. Firstly, the reflection zeros can be extracted based on the response fitting by using the vector fitting technique [52]. Then, two items are considered in the objective function: the magnitude of the S_{11} and reflection zero positions. The objective function can be formulated as

$$F_4 : \text{Minimize}\left\{a_1\cdot\max\left(\sum_{i=1}^{N-1}\max S_{11.\text{dB}}\left(f_{z,i}, f_{z,i+1}\right)-\left(-20\right),0\right) + a_2\cdot\sum_{i=1}^{N}\max\left(\left|f_{z(i)}-CF\right|-BW/2,0\right)\right\} \quad (4)$$

where max $S_{11.\text{dB}}(f_{z(i)}, f_{z(i+1)})$ is the maximum S_{11} values between each two reflection zeros. $f_{z(i)}$ (i = 1, …, N) denotes the extracted reflection zeros in the simulated S_{11} during optimization. CF = 10 (GHz) is the desired center frequency of the filter, BW = 0.1 (GHz) is the desired bandwidth of the filter. The first item aims to minimize the magnitude of the S_{11} to desired value while the second one is to move the reflection zeros into the specified passband. a_1 and a_2 are weights to make the values of two items comparable. In this case, the weights are set as a_1 = 1 and a_2 = 1000.

The characteristic landscapes of four different types of objective functions are shown in Fig. 8-11. For all of the objective functions, the first combination depicts a highly multimodal landscape resulting in a rough landscape with multiple local optima around the global optimum while the second one depicts landscapes with a relatively narrow valley, especially for the first three. The peaks of some pictures, i.e., Fig. 8(b) and Fig. 10. (b) cannot be clearly seen because the valley is too narrow to be recognized by the sampled mesh data. The characteristics of the first two combinations, namely multimodal and narrow, are combined in the third combination for each objective function. We can conclude that microwave filter's distinctive design characteristics is highly multi-modal and the global optimal results is located in a very narrow valley. The roughness of the landscape is affected by the coupling dimensions while the narrowness is affected by the resonator lengths. Further, we can imagine that the landscape is likely to worsen when the filer has a higher-order, narrower bandwidth, and more complex configurations, e.g., cross couplings, multiple modes, multiple bands, and multiple channels. Surprisingly, the 4th objective function (Equ. (4)) smooths the design landscape in a great deal. Hence, reasonable employing features of the filtering response in the objective function can make the design landscape smoother benefiting the convergency in the optimization.

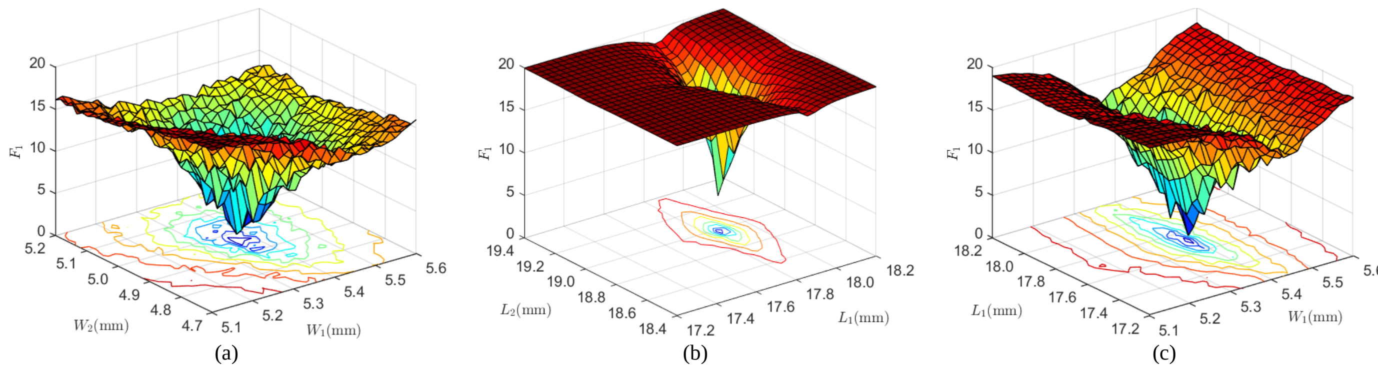

Fig. 8. Characteristic landscape of the objective function F_1 for the three parameter sweeping combinations of (a) W_1 and W_2, (b) L_1 and L_2 and (c) W_1 and L_1.

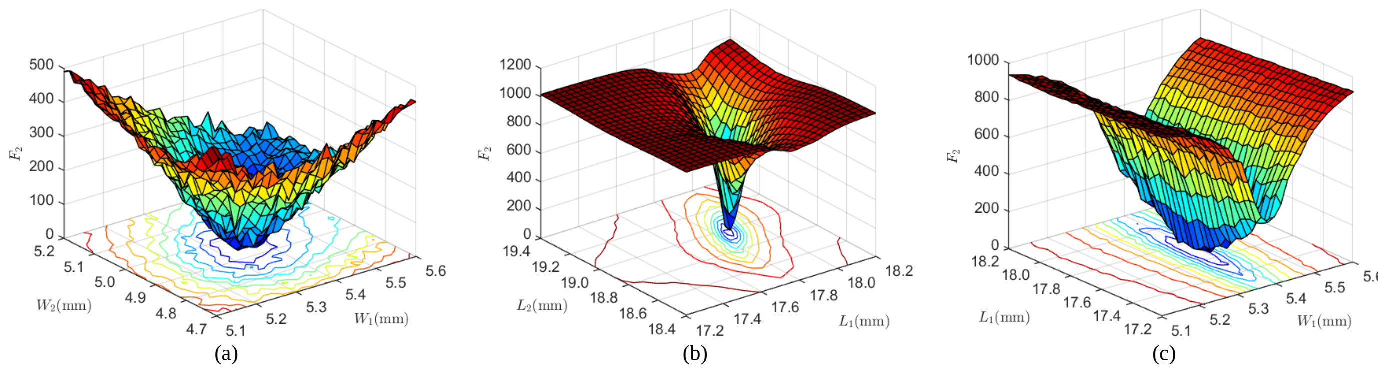

Fig. 9. Characteristic landscape of the objective function F_2 for the three parameter sweeping combinations of (a) W_1 and W_2, (b) L_1 and L_2 and (c) W_1 and L_1.

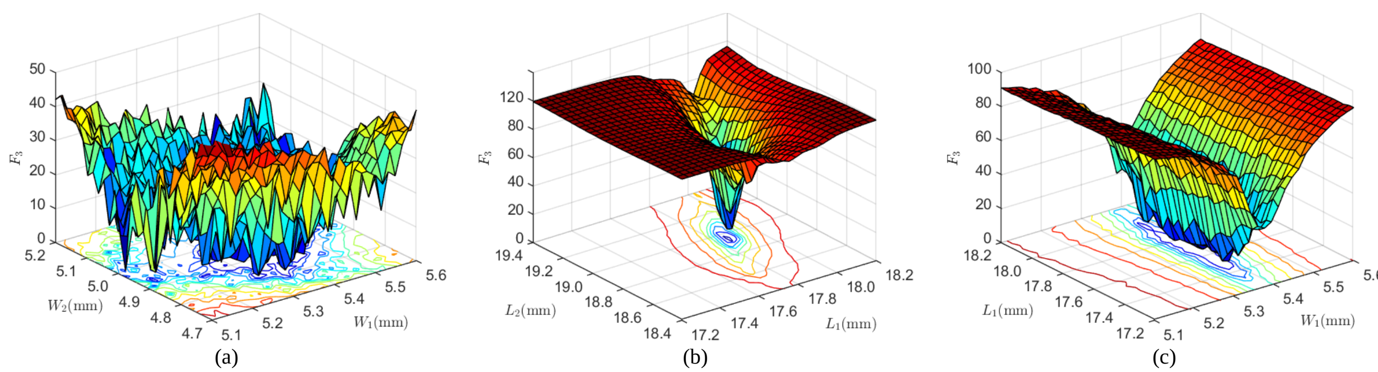

Fig. 10. Characteristic landscape of the objective function F_3 for the three parameter sweeping combinations of (a) W_1 and W_2, (b) L_1 and L_2 and (c) W_1 and L_1.

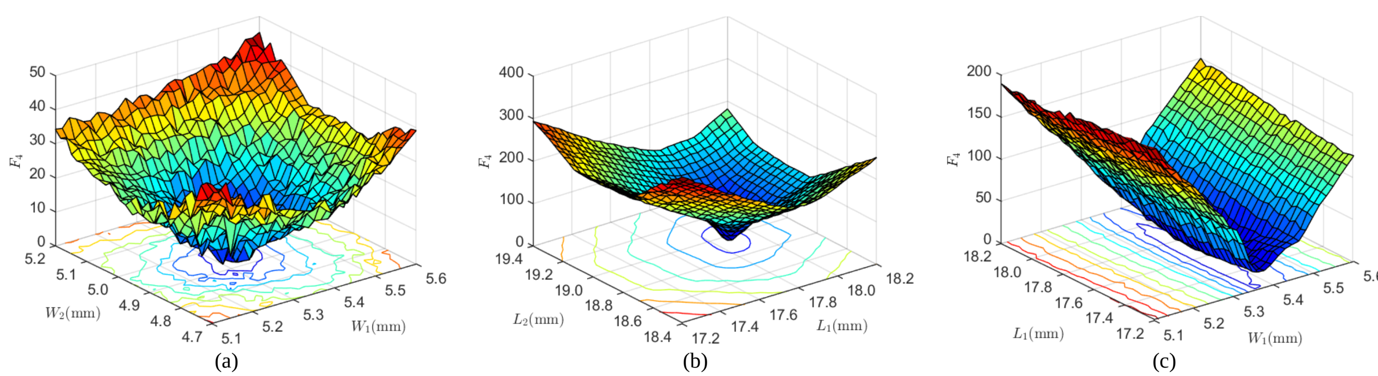

Fig. 11. Characteristic landscape of the objective function F_4 for the three parameter sweeping combinations of (a) W_1 and W_2, (b) L_1 and L_2 and (c) W_1 and L_1.

According to the characteristics of the microwave filter design, it is not all of the available SAO techniques that are employed to make the filter design satisfy specifications. The following challenges, but not limit to, should be taken into account when developing an SAO method for microwave filters: 1) Obtain high quality initial designs or close-to-optimal data set via smart sampling strategies. This can help to narrow the search range and getting close-to-optimal modal. 2) Using filter design knowledge, decompose the entire optimization problem into sub-problems as different types of variables have distinct focuses and sensitivity, e.g., coupling values and resonator lengths. 3) Incorporate "knowledge" (feature zeros) in the objective function or surrogate modeling process. The design landscape will be smoother. 4) Select suitable

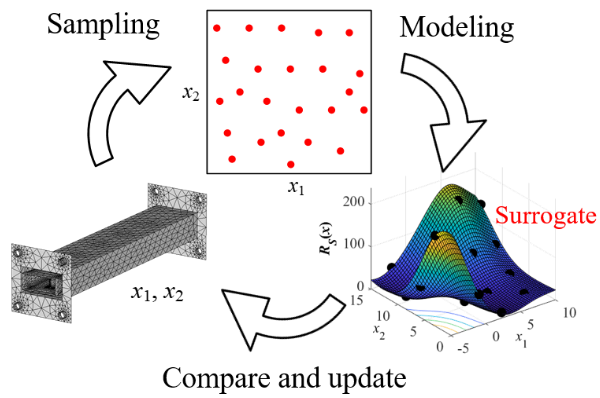

Fig. 12. An illustrative workflow of data-driven surrogate modeling.

optimization methods or frameworks to avoid the optimization trapping into local optima and improve exploitability for narrow valley.

III. AI-ASSISTED SURROGATE MODELING AND OPTIMIZATION TECHNIQUES FOR MICROWAVE FILTER DESIGN

A. Basic concept of surrogate modeling and optimization

The microwave filter design is formulated as an optimization problem as [53]

$$\begin{aligned} \boldsymbol{x}^* &= \arg\min_{\boldsymbol{x}} U\left(\boldsymbol{R}\left(\boldsymbol{x}\right)\right) \\ s.t.\ \ \boldsymbol{x} &\in \left[\boldsymbol{x}_{LB}, \boldsymbol{x}_{UB}\right] \end{aligned} \tag{5}$$

where $\boldsymbol{x} = [x_1, x_2, \ldots, x_n]$ denotes the design variables, where n is the number of the design variables. $\boldsymbol{x}^*$ is the optimal design. $U(\cdot)$ is a form of objection function, $\boldsymbol{R}(\boldsymbol{x})$ is the filter responses. $[\boldsymbol{x}_{LB}, \boldsymbol{x}_{UB}]$ is the design search range. Equation (5) describes directly using a full-wave EM simulation model to solve the optimal solution, which is quite time-consuming. Surrogate-assisted optimization (SAO) is a strategy for reducing the cost of direct optimization. It is formulated as

$$\boldsymbol{x}^* = \arg\min_{\boldsymbol{x}} \boldsymbol{R}_S\left(U\left(\boldsymbol{R}\left(\boldsymbol{x}\right)\right)\right) \tag{6}$$

where $\boldsymbol{R}_S(\cdot)$ is the responses value of constructed surrogate model. The fundamental concept is to optimize a continuously updated surrogate model (low fidelity and fast evaluation) instead of direct optimizing an EM full-wave simulation model (high fidelity and slow evaluation). Theoretically, filters have nature physical surrogates, e.g., polynomial representation, equivalent circuit, coupling matrix. Note that the surrogate should preferably behave in a linear or correlated behavior to the fine model. However, for some complex cases, e.g., dual-mode resonators, cross-couplings, the relationship between the surrogate and fine model will become more complex (nonlinear), it will make the surrogate and its optimization less efficient. To overcome the lack of a physical surrogate model in filter design, machine learning techniques, known as data-driven surrogate models [53], are used to establish the relationship between design variables and design objectives. As demonstrated in Fig. 12, the data-driven surrogate model

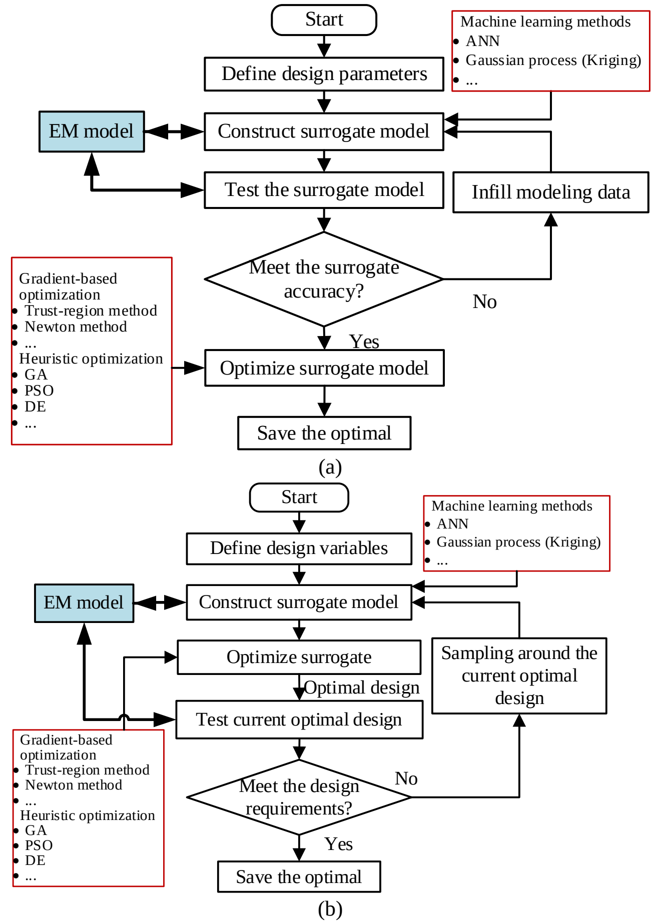

Fig. 13. Illustration of the AI-assisted surrogate modeling and optimization frameworks. (a) The global SAO framework, (b) The local SAO framework.

establishes low-cost mathematical models using a few EM simulation samples. In this process, all of the sampling methods, surrogate modeling methods and optimization frameworks are critical.

Generally, the SAO frameworks can be separated into global SAO framework and local SAO framework. Their flowcharts are given in Fig. 13. The global SAO algorithm [Fig. 13(a)] completes the surrogate model construction and optimization processes separately, maintaining the accuracy of the surrogate model throughout the process. It is expected that once the surrogate model is constructed, it can fully replace the EM simulation model in the design interval to perform the optimization procedure. This method is normally appropriate for filter optimization problems with a small design space, such as when a decent initial design is obtained. The correctness of the surrogate model, demonstrated in Fig. 13 (a), is the most important issue in this approach. The following is a summary of the general procedure of the global SAO framework:

Step G1: Create training samples using relevant experimental approaches;

Step G2: Obtain training data by replicating simulating the proposed high-fidelity model chosen in step 1;

Step G3: Develop surrogate models using selected modeling approaches;

Step G4: Refine the surrogate model;

Step G5: If the target accuracy is met, run the optimizer (local optimizer or global optimizer) and verify the best solution. If not, infill samples and proceed to step G3;

As an opposite of the global SAO framework, local SAO framework is performed as shown in Fig. 13 (b). The following is a summary of the general procedure of the local SAO framework:

Step L1: Design training samples using appropriate experiment methodologies;

Step L2: Obtain training data by simulating the chosen high-fidelity model pre-selected in Step 1;

Step L3: Create surrogate models using modeling techniques (ANN, GPR, etc.);

Step L4: Determine the best surrogate model for optimization and evaluate it.

Step L5: If the target accuracy is met, run the optimization algorithm. Obtain an optimization solution to the current surrogate.

Step L6: Evaluate the obtained solution. If design specification is met, the optimization solution will be saved as the optimal design. If not, then resample around the optimization solution and reconstruct a new surrogate to execute optimization.

It can be noticed that the global SAO framework establishes a global surrogate model prior to optimization to ensure the optimization stability. Therefore, the accuracy requirement of the surrogate model with respect to the entire design variables is relatively high. On the other hand, the local surrogate is built near each design candidate during the optimization phase. The number of sample points in a single local surrogate is obviously less than the one for a global surrogate. However, since the local surrogate is required at each iteration of the optimization process, the local surrogate is updated with the optimization results after each iteration. It also means that the optimizing multiple iterations is challenging.

In the following, the SAO techniques that have been developed in recent years, including smart sampling methods, advanced surrogate modeling methods and effective optimization algorithms and frameworks, are reviewed with their applications.

B. *Smart sampling methods*

Conventional (static) sampling methods widely used for surrogate-assisted microwave component modeling and optimization include full factor sampling (FFS) [54], Monte Carlo sampling (MCS) [55], and Latin hypercube sampling (LHS) [56], etc. These sampling methods focus on improving the uniformity of distributed samples in the design space. Fig. 14 (a)-(c) illustrates these uniform sampling methods in two-dimensional space. In order to evaluate the performance of sampling method, an indicator u called uniformity for sampling method has been proposed [57]. It is defined as the smallest distance between any two samples in the data set:

$$u = \max_{1\le i\le N, i+1\le j\le N}\left(\left\|\boldsymbol{x}^{(i)}-\boldsymbol{x}^{(j)}\right\|^2\right) \tag{7}$$

where N is the sampling number. $\boldsymbol{x}^{(i)}$ and $\boldsymbol{x}^{(j)}$ are the two samples. With a same sampling number and dimension, a larger u denotes better sampling uniformity. Here, we compare these popular uniform sampling methods shown in Fig. 14, including FFS, MCS and LHS. In the comparison, three sampling method are evaluated in the design space of $[-1, \ldots, -1]^d \times [1, \ldots, 1]^d$, where d is the dimensions of the design spaces. The uniformities of these sampling methods are compared in Table III. It can be notice that all classic method can obtain a comparable sampling uniformity, where the commonly used MCS and LHS have better performance. They are all suitable for surrogate modeling.

For microwave components, in certain regions of the design space, the performance with respect to design parameters may be very sensitive. Therefore, "good" samples (close-optimal) nearly satisfying the design specifications may be located in small regions in the design space. If uniform sampling methods are applied, the good samples and the poor samples (which are far from optimal) become unbalanced. Surrogate models based on these unbalanced samples may lead to inefficient optimization. To improve the sampling efficiency, high-quality adaptive sampling methods (ADSs) are sought for surrogate modeling and optimization to improve the sampling efficiency

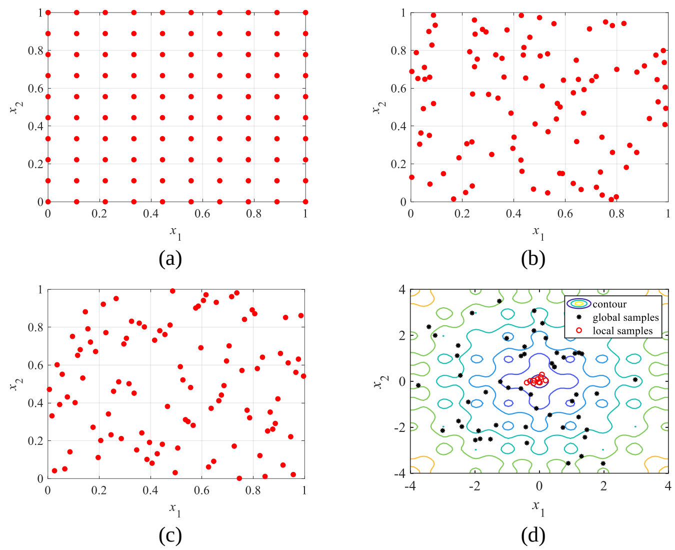

Fig. 14. Illustration of different methods in two-dimensional space, (a) FFS [54], (b) MCS [55], (c) LHS [56] and (d) ADS [57]

TABLE III
UNIFORMITY COMPARISON OF THE SAMPLING METHOD

Sampling method	10 samples	20 samples	50 samples	100 samples
FFS	0.33 (9)*	0.25 (25)*	0.14 (49)*	0.2
MCS	0.30	0.28	0.25	0.25
LHS	0.28	0.27	0.24	0.23

* FFS only has the form of d by d. Therefore, FFS uses close samples to compare another two methods as shown in the brackets.

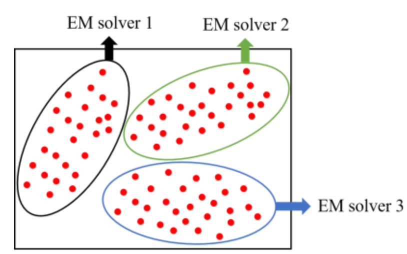

Fig. 15. Illustration of parallel parameter sampling strategy.

TABLE IV
MACHINE LEARNING TECHNIQUES FOR SURROGATE MODELING OF MICROWAVE FILTERS

Machine Learning Methods	Application
Multilayer perceptron neural network (MLP)	Parametric modeling and optimization [65]; Inverse modeling [67]-[68].
Knowledge-based neural network (filter responses "knowledge" + MLP),	Parametric modeling and optimization [69]-[70]; Yield optimization [71]; Yield estimation [72]; Multiphysics modeling and optimization [73]-[75].
Extreme learning machine (ELM)	Filters optimization [77].
Support vector machine (SVM)	Filter Tuning [63], [83] Inverse modeling [64] Parametric modeling and optimization [82].
Gaussian process regression （also called Kriging）	Filters optimization [51]; Yield optimization [83]; Diplexer optimization [85].
Radial basis function neural network (RBFNN)	Parametric modeling [78]; Yield optimization [79]
Deep neural network (DNN)	Parameter extraction [80] Filter tuning [89]
Graph neural network (GNN)	Automatic design [86]
Deep belief network (DBN)	Inverse modeling [87]
Convolutional Neural Network (CNN)	Filter tuning [88]-[89]

[58]-[59]. An illustrative sampling example is shown in Fig. 14(d). The methods combine local sampling and global sampling to construct more accurate data-driven surrogate model for microwave filters [58]. Clearly, ADSs cover whole design space but also focuses on area with "good" samples. For another, the design space can be divided into multiple subspaces according to the characteristics of design variables as shown in Fig. 15. Then, sampling process is implemented in parallel by multiple EM solvers with same configuration, which can improve the sampling efficiency [60]-[61] and facilitate the following modeling process. Parallel local sampling strategy can increase the exploitation ability near the potential optimal solution in each optimization process [61]. The microwave filter optimization will avoid local minimum and keep a high convergence rate.

C. *Advanced surrogate modeling methods*

Various surrogate modeling techniques are implemented to reduce the computational cost of microwave filter modeling and the SAO process, e.g., polynomial regression [62], support vector machine [63]-[64], artificial neural networks (ANN) [65] and Gaussian process regression (GPR) [51]. Various surrogate modeling (machine learning) techniques with their application in microwave filters are summarized in Table IV. Some key features of some classic modeling methods are discussed in the following.

1) Artificial neural networks (ANN):

MLP is a basic artificial neural network (ANN) method used in microwave filter parametric modeling [66]-[75]. It is

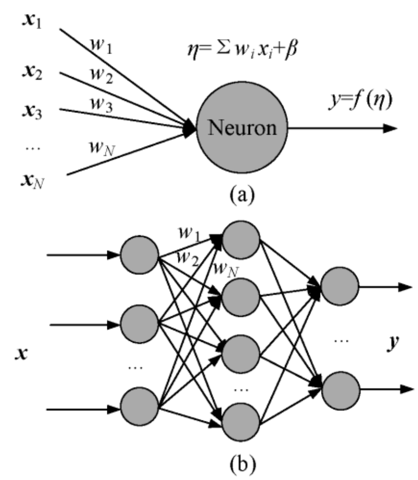

Fig. 16. The Structure of the MLP.

effective at modeling nonlinear functions [76]. The MLP is a fully connected ANN model and its basic element is a neuron shown in Fig. 16(a), where w_i, i=1, 2, …, N are weights, β is a bias, and $f(\eta)$ is an activation function. Then, MLP is constructed by connections of artificial neurons with different weights as shown in Fig. 16 (b), the structure of the network has three parts: input, output and hidden layers, and can be either forward or backward. In the forward mode, data will be transferred through the network layer by layer until it reaches the output layer. Finally, the weight sum is transferred by the activation function to the output. Backward mode (backpropagation of MLP) optimizes the weights and bias to minimize the error between desired and predicted outputs. This process is also known as the training process. The surrogate will be successful defined when the discrepancy is lowered to an acceptable threshold. Then, based on MLP, more advanced NN methods are developed as new machine learning methods for parametric modeling of microwave filter. Extreme learning machine (ELM) is a single-hidden layer feed-forward neural network (SLFNN) which is much simpler than the MLP [77]. ELM transform the output from SLFNN into a matrix calculation and this speed up the training process [77]. However, its accuracy is not as good as the MLP training. Radial basis function (RBF) neural network utilizes the Radial basis function as the activation function [78]-[79]

$$\varphi(\boldsymbol{x}) = \exp\left(-\frac{\|\boldsymbol{x}-\boldsymbol{c}\|^2}{2\sigma^2}\right) \tag{8}$$

where $\boldsymbol{c}$ are radial basis centers. Deep neural network is the MLP with more than 2 hidden layers [80].

2) Support vector machines (SVM):

SVM is mainly applied in classification [81]. It can predict the microwave filter designs satisfying or dissatisfying specified goals. As a binary classifier, the SVM aims to search a hyperplane to separate two categories. The criteria for the best hyperplane are: 1) The objects belong to correct categories and 2) the margin (the distance between nearest data point (two category) and the hyperplane) is maximized. By solving this constrained optimization, a hyperplane can be obtained and it will be used as classifier for new objects. The above

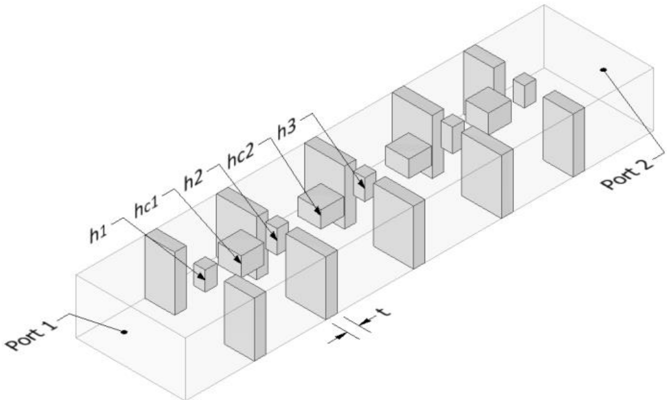

Fig. 17. The geometry of the four-pole filter example.

TABLE V
PERFORMANCE COMPARISON OF DIFFERENT SURROGATE MODELING METHODS

	Modeling Error			Time Cost (minute)		
	MLP	RBFNN	GPR	MLP	RBFNN	GPR
S11	2.976	2.755	2.309	1.055	0.108	0.278
S21	0.453	0.270	0.276	1.064	0.182	0.683

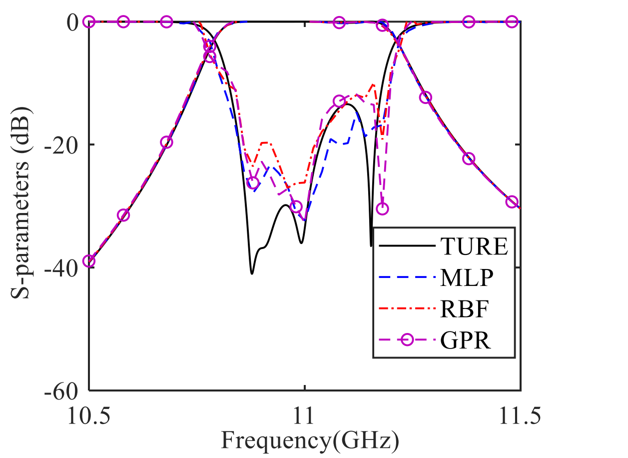

Fig. 18. Comparison of the predicted responses by different surrogates and the true simulated responses.

constrained optimization problem is given as follows:

$$\begin{aligned} &\min \frac{1}{2}\varpi^T\varpi + \kappa\sum\theta_i \\ &s.t.\ \ l_i\left(\varpi^T\phi(\boldsymbol{h}_i)^T + b_s\right) \geq 1-\theta_i \\ &\qquad \theta_i \geq 0 \end{aligned} \tag{9}$$

where ϖ is the normal vector to the hyperplane. $\kappa > 0$ is a penalty coefficient of the error term. The slack variables θ_i refer to the degree of classification error of sample $\boldsymbol{h}_i$. For more details can be found in [81].

3) Gaussian process regression (GPR):

The GPR, also known as kriging method [53], establishes a surrogate for N samples $\boldsymbol{X} = (\boldsymbol{x}^1, \ldots, \boldsymbol{x}^N)$ and their corresponding responses $\boldsymbol{Y} = (\boldsymbol{y}^1, \ldots, \boldsymbol{y}^N)$. The GPR assumes that the random variables satisfy a multivariate Gaussian distribution with mean μ and variance σ^2. The Gaussian correlation function calculate the correlation between two samples ($\boldsymbol{x}^{(i)}$ and $\boldsymbol{x}^{(j)}$) in the form:

$$\boldsymbol{Z}\left(\boldsymbol{x}^{(i)}, \boldsymbol{x}^{(j)}\right) = \exp\left(-\sum_{l=1}^{d}\boldsymbol{\theta}_l\left|\boldsymbol{x}_l^{(i)} - \boldsymbol{x}_l^{(j)}\right|^2\right) \tag{10}$$

where d is the dimension of $\boldsymbol{x}$, $\boldsymbol{\theta}_l$ is the so-called scale parameters which determines how fast the correlation decreases when $\boldsymbol{x}^{(i)}$ moves in the l-direction and l is the index of vectors. The optimal values $\hat{\mu}$ and $\hat{\sigma}^2$ can be determined by maximized likelihood estimation, they can be solved by

$$\hat{\mu} = \left(\boldsymbol{I}^T\boldsymbol{Z}^{-1}\mathbf{Y}\right)^{-1}\boldsymbol{I}^T\boldsymbol{Z}^{-1}\mathbf{Y} \tag{11}$$

$$\hat{\sigma}^2 = \frac{1}{N}\left(\mathbf{Y} - \boldsymbol{I}\hat{\mu}\right)^T\boldsymbol{Z}^{-1}\left(\mathbf{Y} - \boldsymbol{I}\hat{\mu}\right) \tag{12}$$

where $\boldsymbol{I}$ is a unit row vector and $\boldsymbol{Z}_{ij} = \boldsymbol{Z}(\boldsymbol{x}^{(i)}, \boldsymbol{x}^{(j)})$ is the correlation matrix. Based on the GP model, the predicted value $\hat{y}(\boldsymbol{x}^*)$ is

$$\hat{y}\left(\boldsymbol{x}^*\right) = \hat{\mu} + \mathbf{z}_0^{\ T}\boldsymbol{Z}^{-1}\left(\mathbf{Y} - \boldsymbol{I}\hat{\mu}\right) \tag{13}$$

And the mean square error $\hat{s}^2(\boldsymbol{x}^*)$ is expressed as

$$\hat{s}^2\left(\boldsymbol{x}^*\right) = \hat{\boldsymbol{\sigma}}^2\left[1 - \mathbf{z}_0^{\ T}\boldsymbol{Z}^{-1}\mathbf{z}_0 + \left(1 - \mathbf{z}_0^{\ T}\boldsymbol{Z}^{-1}\mathbf{z}_0\right)^2\left(\boldsymbol{I}^T\boldsymbol{Z}^{-1}\boldsymbol{I}\right)^{-1}\right] \tag{14}$$

where $\mathbf{z}_0 = [\boldsymbol{Z}(x^*, x^1), \ldots, \boldsymbol{Z}(x^*, x^N)]^T$. An infill method is utilized to improve the accuracy of the GP model. New sample $\boldsymbol{x}^{new}$ is obtained by

$$\boldsymbol{x}^{new} = \arg\min_{\boldsymbol{x}}\left(\hat{y}(\boldsymbol{x}) - w\cdot\hat{s}(\boldsymbol{x})\right) \tag{15}$$

where w is responsible for balancing the exploitation ($w \rightarrow 0$) and exploration ($w \rightarrow \infty$).

MLP, RBF and GPR are classic modeling methods for regressing the relationship between the design variables and S-parameters. Here, we employ an X-band four-pole waveguide filter shown in Fig. 17 to evaluate the different surrogate modeling methods. The filter structure is symmetric and the design variables are $\boldsymbol{x}$ = [h_1, h_2, h_3, hc_1, hc_2] (mm). The thickness for all the coupling window is set to 2mm. The design objective is to minimize the return loss within the passband 10.85-11.15GHz. The sampling is performed using MCS around a design candidate x_0 = [3.335, 4.044, 3.588, 3.299, 2.971] and sampling range is [x_0 −0.1, x_0 +0.1].

Three modeling methods, MLP, RBFNN and GPR are compared. Both MLP and RBFNN have one hidden layer with 15 neurons. 150 samples are used for modeling and 50 for testing. Predicted responses $\boldsymbol{S}_{11.pre}$ and $\boldsymbol{S}_{21.pre}$ from three surrogate and responses of testing samples $\boldsymbol{S}_{11.test}$ and $\boldsymbol{S}_{21.test}$ are used to evaluate the modeling accuracy. The modeling errors of S11 and S21 are calculated by

$$error\left(S_{11}\right) = \frac{1}{N}\frac{1}{M}\sum_{n=1}^{N}\sum_{m=1}^{M}\left|\boldsymbol{S}_{11.pre}^{n,m} - \boldsymbol{S}_{11.test}^{n,m}\right| \tag{16}$$

$$error\left(S_{21}\right) = \frac{1}{N}\frac{1}{M}\sum_{n=1}^{N}\sum_{m=1}^{M}\left|\boldsymbol{S}_{21.pre}^{n,m} - \boldsymbol{S}_{21.test}^{n,m}\right| \tag{17}$$

where M is the sampled frequency points on S-parameter responses. N is the number of testing samples. The modeling errors for three modeling methods are compared in Table V and the predicted responses by using different modeling methods compared with the true responses are shown in Fig. 18. According to the comparison, we can notice that these modeling methods with a default setting have a certain ability

Table VI
CHARACTERISTICS OF DIFFERENT CLASSIC SURROGATE MODELING METHODS

	MLP	RBFNN	GPR
Learning mode	Supervised learning	Semi-Supervised learning	Supervised learning
Approximation mode	Global approximation	Local approximation	Global approximation
Features	Simple structure, Unsensitivity to noise data	Low-cost modeling Sensitivity to noise data	Provide uncertainty analysis

in parametric modeling. To increase the modeling accuracy, we should consider narrowing the sampling range and increasing the number of samples. RBFNN has a fast speed than the MLP and GPR has better performance in both speed and accuracy. This is mainly because its uncertainty analysis ability. The characteristics of the above modeling methods are listed in Table VI.

The state-of-the-art surrogate modelling method for microwave filters is the multiple features assisted surrogate, e.g., neuro-transfer function surrogate [89]-[94]. This method first extract feature zeros and poles from EM simulation response. Then, the extracted feature zeros are employed in the surrogate modeling. The feature-based EM optimization can move the simulated passband into the range of design specifications. As proofed in section II (c), the surrogate model based on feature-based objective function will smooth the design landscape which avoid the optimization trapping into local optima. Not only in EM optimization, the feature-assisted surrogate can also be utilized in filter tuning [82], yield estimation [72]-[73], diplexer optimization [84], etc.

Other than directly implementing one surrogate, multi-fidelity strategy is often employed based on multiple fidelity modelling framework [62], [90], co-kriging method [95] and also SM techniques. In the multi-fidelity surrogate modeling strategy, the surrogate is constructed and optimized based on the multiple cascaded low-fidelity models and then the optimization results of low-fidelity model are calibrated to high-fidelity model. This aims to increase the correlation between multiple fidelity models. The model correction can be formulated as

$$\boldsymbol{R}_S(\boldsymbol{x}) = \boldsymbol{A} \cdot \boldsymbol{R}_c(i, \boldsymbol{x}) \tag{18}$$

where $\boldsymbol{R}_S(\boldsymbol{x})$ is the corrected surrogate model and $\boldsymbol{A}$ denotes a diagonal correction matrix. $\boldsymbol{R}_c(\boldsymbol{x}^{(i)})$ is the ith low-fidelity model. It can be assumed that the surrogate model established using low-fidelity samples is time-saving and the high-fidelity model provides extra information to save the accuracy. For a surrogate built on EM simulations at a certain fidelity, the output SM method may be used to improve the performance of the surrogate [95]. These methods usually only correct the linear error between the surrogate model and the EM simulation model. When one low-fidelity model has a non-linear relation to the high-fidelity model, more continuous fidelity models should be required [62]. The correction matrix can be obtained by

$$\boldsymbol{A}^* = \arg\min_{A} \sum_{i=1}^{n} \left\| \boldsymbol{R}_f(\boldsymbol{x}^{(i)}) - \boldsymbol{A} \cdot \boldsymbol{R}_c(\boldsymbol{x}^{(i)}) \right\|^2 \tag{19}$$

where $\boldsymbol{R}_f(\boldsymbol{x}^{(i)})$ is the fine model using $\boldsymbol{x}^{(i)}$. Therefore, the corrected surrogate can be obtained by

$$\boldsymbol{R}_S(\boldsymbol{x}^{(i)}) = \boldsymbol{R}_c\left(\boldsymbol{x}^{(i)}\right) + \left[\boldsymbol{R}_f(\boldsymbol{x}^{(i)}) - \boldsymbol{R}_c(\boldsymbol{x}^{(i)})\right] \tag{20}$$

The correction term $\boldsymbol{R}_f(\boldsymbol{x}^{(i)}) - \boldsymbol{R}_c(\boldsymbol{x}^{(i)})$ has to be a zero-order consistency between the two fidelity models.

D. Surrogate optimization

Besides the learning EM-behavior of microwave filters in surrogate modeling, the optimization frameworks are also important part of the SAO filter design method. Either local optimizers or heuristic global optimizers are implemented. The widely used local optimizers include trust region algorithm [96]-[98], newton and quasi-newton methods [99], Nelder-Mead simplex algorithm [106], and Homotopy optimization [101]. The global optimizers for microwave filters include Harris Hawks algorithm [102]-[103], genetic algorithm (GA) [104], particle swarm optimizer (PSO) [105], and self-adaptive differential evolution (DE) [51], [84]. Local optimizer and global optimizer have different features in searching optimal values. Both of the optimizers have to work with surrogate in the optimization frameworks.

The optimizer in SAO should be selected based on the characteristics of the design landscape, namely according to our analysis in Section II-D. Generally speaking, the local optimizer depends on good starting point and is more suitable for the design space with narrow and smooth landscape. Otherwise, local optimizer is easily trapped into local optima. On the other, global optimizer should be used when the starting point is unclear and suitable for the design landscape is multimodal. It is worth to note that they require appropriate adjustments to adapt to the characteristics of the microwave designs

Many strategies in surrogate modeling are employed facilitating the following optimization process. For example, the local optimizer, e.g., trust region algorithm, is widely investigated in many microwave filter design examples [96]-[98]. To avoid being trapped in local optima, the local optimizers are assisted by "knowledge" in the surrogate modeling and start from a good initial design. To explore the filter optimization with a large design space (optimization with a large number of design variables or starting point is far from optimal), such a problem is solved by decomposition using trust region optimization method [96]. Some work employs a heuristic global optimizer to explore the filter design with a large search space [100]-[103]. The state-of-the-art SAO method is multiple feature-assisted SAO based on trust region optimization [89]-[94]. As proofed in Section II-D and III-C, knowledge learned from transfer function of microwave filters can guide the trust region optimization to efficiently design microwave filters.

The existed optimizers and their applications are listed and compared in Table VII.

TABLE VII
OPTIMIZERS IN SAO FRAMEWORKS FOR MICROWAVE FILTER DESIGN

Optimization Method	Reference	Application
Local algorithms	Trust-region algorithm [92]-[94],[97]-[98]	4th order waveguide filter (5 variables) 4th order waveguide filter using the piezo actuator multiphysics optimization (6 variables) 5th order waveguide filter yield optimization (3 variables) 5th order waveguide filter (9 variables)
	Gradient-based Quasi-Newton algorithm [99]	5th order waveguide filter (9 variables)
	Homotopy optimization [101]	5th order waveguide filter with 6 variables; 5th order filter with one frequency dependent coupling with 12 variables
Global algorithms	Harris Hawks algorithm [102]-[103]	4th-order dielectric filter (7 variables) 4th-order cross-coupled filter (6 variables)
	GA [104]	3rd order LC filter (6 variables)
	PSO [105]	8th order dielectric filter (8 variables)
	Self-adaptive DE [51], [84]	6th order waveguide filter (5 variables). 8th order microstrip filter (12 variables). 10th order waveguide diplexer (22 variables); 8th order waveguide diplexer (23 variables)
Hybrid algorithm	GA algorithm + Nelder-Mead simplex algorithm [106], [107]	4th order ridged waveguide filter (9 variables) 4th order dielectric filter (7 variables)
	Gradient Particle Swarm [108]	4th order waveguide filter (6 variables)

IV. APPLICATIONS AND EMERGING TRENDS OF MICROWAVE FILTER DESIGN

The proposed SAO filter design methods aim to deal with the existing resource intensive problems in the microwave filter designs and also drive new type of microwave filter structures. They are discussed in the following.

A. *Problem-oriented SAO EM design methods*

Using advanced methods, the existing problems in the microwave filter design are addressed in an efficient and reliable way. For example, with the requirement of 5G and mmWave applications, the fabricated microwave filter with good performance is desired. However, the filter responses are very sensitivity to the fabrication errors. High qualified fabricated filters improved by yield (ratio of the number of qualified fabricated filters to the total number of fabricated filters) optimization are concerned. The challenges mainly come from the yield estimation which requires a large amount of EM simulation which is computationally expensive. Therefore, machine learning methods are widely employed such as ANN [72], [98] and polynomial chaos [109]-[112]. Recently, a new method called surrogate model-assisted evolution algorithm for filter optimization (Y-SMEAFO) has been proposed for filter design with high dimensional parameters [79]. Quadratic support vector machine-based classification and radio basis function neural network -based regression using extracted features are designed to realize high-accurate surrogate models. With global optimization, the Y-SMEAFO realized filter yield optimization with more than 10 sensitivity design variables and signification yield improvement (30%-40%) for a direct coupled filter with 11 variables and a cross-coupled filter with 14 variables.

In this case, we can notice that despite that various EM optimization techniques have been proposed, efficient SAO frameworks are still necessary to address the increasingly emerging problems in microwave filter designs. The challenges can be found in the accurate modeling the filter design with higher dimensional variables (the number of design variables larger than 20), complex structures, i.e., cross-couplings, multiple modes, multiple bands and multiple channels and integrated filtering components, i.e., filter antenna [117], filtering amplifier [118]-[119] and so on.

B. *SAO techniques for novel design applications*

Combining new simulation techniques and fabrication techniques, SAO techniques drive novel filter design routines and structures. The work in [85] proposes a graph neural network (GNN) that learns how to simulate electromagnetic properties of the distributed circuits of microwave filters. The GNN model is trained based on the capture pictures of various planar filters with different topology and size. Then the trained GNN can replace the EM simulators and automated microwave filter design process can be achieved. The automated generated circuits are intrinsically different from regular standard topology of microwave filters, which expand the design capability [85]. Another example is shape deformation technique for geometry optimization of microwave filter [113]-[114]. The method is performed based on computer graphics applications which is used for object manipulation. Firstly, a set of control points are defined around the cavity resonator with regular shape, e.g., rectangular resonator. Then the coordinates of the points are controlled and shifted. Accordingly, the regular shape will be deformed based on the performance optimization of the resonator, e.g., Q factor and spurious performance. Finally, assisted with 3D EM simulation-based optimization, the filters are designed based on the deformed resonators following the process introduced in Section II. This method offers a greater freedom than the conventional resonator. Based on 3D printing fabrication technique, the filters with higher performance can be realized. Also, some other techniques, e.g., topology optimization [115], model order reduction [116] and Multiphysics simulation-based optimization [73]-[75], have been investigated for filter design with new design routine and novel structures.

V. CONCLUSION

Focusing on EM design methodologies for microwave filter designs, this paper illustrates the AI-based design flow for microwave filter designs in detail. Three levels of AI-based EM design techniques for microwave filters are first defined and explained in this paper. To better understand the challenges in microwave filter design and proper application of AI techniques, design "knowledge" and characteristics landscape are investigated and summarized using study cases. Based on the analysis of filter characteristics, the reasons for adjustments in AI techniques are clearer recommended. Then, the present state-of-the-art AI techniques in current EM-simulation based design for microwave filters are reviewed with a focus on smart sampling techniques, advanced surrogate modeling techniques and effective optimization algorithms and frameworks, as well as their applications. Moreover, an outlook for the future study direction is proposed based on the discussion of some recent emerging research works. In a nutshell, AI-based design techniques have been evolved into a general design procedure rather than an optimization tool in microwave filter designs. More useful and powerful AI design techniques will be investigated in the future as we move closer to a full design automation. The authors expect that the discussions in this manuscript would be helpful to both CAD researchers and microwave filter designers.

REFERENCES

[1] K. Wu, L. Zhu, and R. Vahldieck, "Microwave passive components", *The Electrical Engineering Handbook*, Academic Press, 2004.

[2] R. J. Cameron, C. M. Kudsia, and R. R. Mansour, *Microwave filters for communication systems: fundamentals, design, and applications*. Wiley-Interscience, 2007.

[3] J. -S. G. Hong and M. J. Lancaster, *Microstrip Filters for RF/Microwave Application*, vol. 167. Hoboken, NJ, USA: Wiley, 2004.

[4] F. De Paolis, "Satellite Filters for 5G/6G and Beyond," *2021 IEEE MTT-S International Microwave Filter Workshop (IMFW)*, 2021, pp. 148-150.

[5] D. Liang, X. Zhang, B. Yang and D. Young, "Overview of Base Station Requirements for RF and Microwave Filters," *2021 IEEE MTT-S International Microwave Filter Workshop (IMFW)*, 2021, pp. 46-49.

[6] L. Balewski, M. Baranowski, and M. Jasinski, et. al.,"Electromagnetic simulation with 3D FEM for design automation in 5G era," *ZTE Communications*, vol. 18, no. 3, pp. 42–48, Sept. 2020.

[7] S. Shin and S. Kanamaluru, "Diplexer design using EM and circuit simulation techniques," *IEEE Microw. Mag.*, vol. 8, no. 2, pp. 77-82, April 2007.

[8] R. V. Snyder, G. Macchiarella, S. Bastioli, and C. Tomassoni, "Emerging Trends in Techniques and Technology as Applied to Filter Design," *IEEE J. Microwaves*, vol. 1, no. 1, pp. 317-344, Jan. 2021.

[9] G. Macchiarella and S. Tamiazzo, "Novel approach to the synthesis of microwave diplexers," *IEEE Trans. Microw. Theory Techn.*, vol. 54, no. 12, pp. 4281–4290, Dec. 2006.

[10] G. L. Matthaei, L. Young, and E. M. T. Jones, *Microwave filters, impedance-matching networks, and coupling structures*. Norwood, MA: Artech House, 1980, ch. 8.

[11] R. Levy, "Theory of direct-coupled-cavity filters," *IEEE Trans. Microw. Theory Techn.*, vol. 15, no. 6, pp. 340-348, June. 1967.

[12] G. Macchiarella, "An original approach to the design of bandpass cavity filters with multiple couplings," *IEEE Trans. Microw. Theory Tech.*, vol. 45, no. 2, pp. 179–187, Feb. 1997.

[13] D. Swanson and G. Macchiarella, "Microwave filter design by synthesis and optimization," *IEEE Microw. Mag.*, vol. 8, no. 2, pp. 55-69, April 2007.

[14] G. C. Temes and D. A. Calahan, "Computer-aided network optimization the state-of-the-art," *Proc. IEEE*, vol. 55, no. 11, pp. 1832–1863, Nov. 1967.

[15] J. W. Bandler et al., "Space mapping: The state of the art," *IEEE Trans. Microw. Theory Techn.*, vol. 52, no. 1, pp. 337–361, Jan. 2004.

[16] J. Bandler, "Space Mapping-Have You Ever Wondered About the Engineer's Mysterious "Feel" for a Problem? [Speaker's Corner]," *IEEE Microw. Mag.*, vol. 19, no. 2, pp. 112-122, March-April 2018.

[17] J. E. Rayas-Sánchez, "Power in simplicity with ASM: Tracing the aggressive space mapping algorithm over two decades of development and engineering applications," *IEEE Microw. Mag.*, vol. 17, no. 4, pp. 64–76, Apr. 2016.

[18] J. W. Bandler, Q. S. Cheng, N. Georgieva and M. A. Ismail, "Implicit space mapping optimization exploiting preassigned parameters," *IEEE Trans. Microw. Theory Techn.*, vol. 52, no. 1, pp. 378–385, Jan. 2004.

[19] M. H. Bakr, J. W. Bandler, M. A. Ismail, J. E. Rayas-Sanchez, and Qi-Jun Zhang, "Neural space-mapping optimization for EM-based design," *IEEE Trans. Microw. Theory Techn.*, vol. 48, no. 12, pp. 2307-2315, Dec. 2000.

[20] J. W. Bandler, M. A. Ismail, J. E. Rayas-Sánchez, and Q. J. Zhang, "Neural inverse space mapping (NISM) for EM-based microwave design," *Int. J. RF Microw. Comput.-Aided Design*, vol. 13, no. 2, pp. 136–147, Mar. 2003.

[21] J. E. Rayas-Sánchez, "EM-based optimization of microwave circuits using artificial neural networks: The state of the art," *IEEE Trans. Microw. Theory Techn.*, vol. 52, no. 1, pp. 420–435, Jan. 2004.

[22] C. Zhang, F. Feng, V.-M.-R. Gongal-Reddy, Q. J. Zhang, and J. W. Bandler, "Cognition-driven formulation of space mapping for equal-ripple optimization of microwave filters," *IEEE Trans. Microw. Theory Techn.*, vol. 63, no. 7, pp. 2154–2165, Jul. 2015.

[23] C. Zhang, W. Na, Q. J. Zhang, and J. W. Bandler, "Fast yield estimation and optimization of microwave filters using a cognition-driven formulation of space mapping," *in Proc. IEEE MTT-S Int. Microw. Symp.*, May 2016, pp. 1–4.

[24] C. Zhang, F. Feng, Q. Zhang and J. W. Bandler, "Enhanced cognition-driven formulation of space mapping for equal-ripple optimisation of microwave filters," *IET Microw. Antennas Propag.*, vol. 12, no. 1, pp. 82–91, Jan 2018.

[25] C. Zhang, J. Jin, Z. Zhao and Q. Zhang, "Cognition-driven formulation of space mapping for reducing gain variation of antennas," *in Proc. IEEE MTT-S Int. Conf. Numer. Electromagn. Multiphys. Model. Opt.*, Aug. 2018, pp. 1–3.

[26] Q. S. Cheng, J. W. Bandler and J. E. Rayas-Sánchez, "Tuning-aided implicit space mapping," *Int. J. RF Microw. Comput.-Aided Design*, vol. 18, no. 5, pp. 445–453, Sep. 2008.

[27] J. C. Rautio, "Shortening the design cycle," *IEEE Microw. Mag.*, vol. 9, no. 6, pp. 86–96, Dec. 2008.

[28] S. Koziel, J. Meng, J. W. Bandler, M. H. Bakr and Q. S. Cheng, "Accelerated microwave design optimization with tuning space mapping," *IEEE Trans. Microw. Theory Techn.*, vol. 57, no. 2, pp. 383–394, Feb. 2009.

[29] Q. S. Cheng, J. W. Bandler and S. Koziel, "Space mapping design framework exploiting tuning elements," *IEEE Trans. Microw. Theory Techn.*, vol. 58, no. 1, pp. 136–144, Jan. 2010.

[30] Q. S. Cheng, J. C. Rautio, J. W. Bandler and S. Koziel, "Progress in simulator-based tuning—The art of tuning space mapping [application notes]," *IEEE Microw. Mag.*, vol. 11, no. 4, pp. 96–110, Jun. 2010.

[31] J. C. Rautio, "EM filter design success: The fast way," Microw. J., Feb. 2015. [Online]. Available: https://www.microwavejournal.com/articles/23813-em-filter-design-success-the-fast-way

[32] J. C. Rautio, "Tuning ports in the middle of resonators," *in Proc. IEEE MTT-S Int. Microw. Symp.*, Jun. 2017, pp. 1509–1511.

[33] D. Swanson, "Port tuning a microstrip-folded hairpin filter [application notes]," *IEEE Microw. Mag.*, vol. 21, no. 4, pp. 18–28, Apr. 2020.

[34] M. A. Ismail, D. Smith, A. Panariello, Ying Wang, and Ming Yu, "EM-based design of large-scale dielectric-resonator filters and multiplexers by space mapping," *IEEE Trans. Microw. Theory Techn.*, vol. 52, no. 1, pp. 386-392, Jan. 2004.

[35] Z. -C. Hao, X. -P. Huo, W. -Q. Ding and W. Hong, "Efficient Design of Compact Contiguous-Channel SIW Multiplexers Using the Space-Mapping Method," *IEEE Trans. Microw. Theory Techn.*, vol. 63, no. 11, pp. 3651-3662, Nov. 2015.

[36] J. E. Rayas-Sánchez, S. Koziel, and J. W. Bandler, "Advanced RF and Microwave Design Optimization: A Journey and a Vision of Future Trends," *IEEE Microw. Mag.*, vol. 1, no. 1, pp. 481-493, Jan. 2021.

[37] M. Guglielmi, "Simple CAD procedure for microwave filters and multiplexers," *IEEE Trans. Microw. Theory Techn.*, vol. 42, no. 7, pp. 1347-1352, 1994.

[38] J.T. Alos, M. Guglielmi, "Simple and effective EM-based optimization procedure for microwave filters", *IEEE Trans. Microw. Theory Techn.*, vol. 45, no. 5, pp. 856-858, 1997.

[39] R. J. Cameron, "Advanced coupling matrix synthesis techniques for microwave filters", *IEEE Trans. Microwave Theory Tech.*, vol. 51, pp. 1-10, Jan. 2003.

[40] G. Macchiarella, "Accurate synthesis of in-line prototype filters using cascaded triplet and quadruplet sections", *IEEE Trans. Microwave Theory Tech.*, vol. 50, no. 7, pp. 1779-1783, July 2002.

[41] S. Amari, "Synthesis of cross-coupled resonator filters using an analytical gradient-based optimization technique," *IEEE Trans. Microw. Theory Techn.*, vol. 48, no. 9, pp. 1559-1564, Sept. 2000.

[42] X. Luo, B. Yang, and H. J. Qian, "Adaptive Synthesis for Resonator-Coupled Filters Based on Particle Swarm Optimization," *IEEE Trans. Microw. Theory Techn.*, vol. 67, no. 2, pp. 712-725, Feb. 2019.

[43] B. Liu, H. Yang, and M. J. Lancaster, "Synthesis of Coupling Matrix for Diplexers Based on a Self-Adaptive Differential Evolution Algorithm," *IEEE Trans. Microw. Theory Techn.*, vol. 66, no. 2, pp. 813-821, Feb. 2018.

[44] Y. Yu, B. Liu, Y. Wang, M. J. Lancaster, and Q. S. Cheng, "A general coupling matrix synthesis method for all-resonator diplexers and multiplexers," *IEEE Trans. Microw. Theory Techn.*, vol. 68, no. 3, pp. 987-999, Mar. 2020.

[45] M. Caenepeel, F. Seyfert, Y. Rolain and M. Olivi, "Parametric modelling of the coupling parameters of planar coupled-resonator microwave filters," *in 2015 European Microwave Conference (EuMC), Paris, France*, 2015, pp. 538-541.

[46] M. Caenepeel, F. Ferranti and Y. Rolain, "Efficient and automated generation of multidimensional design curves for coupled-resonator filters using system identification and metamodels," *2016 13th International Conference on Synthesis, Modelling, Analysis and Simulation Methods and Applications to Circuit Design (SMACD)*, 2016, pp. 1-4.

[47] L. Balewski, A. Lamecki, and M. Mrozowski, "Multivariate models of inter-resonator couplings and their application in filter design," *in XXVIIIth General Assembly of International Union of Radio Science (URSI)*, October 2005.

[48] O. Glubokov and S. Koziel, "Automated inverse design of bandpass filters with invariable layout through linear approximation of physical dimensions," *2014 44th European Microwave Conference (EuMC)*, 2014, pp. 1064-1067.

[49] L. Balewski and M. Mrozowski, "Applications of Surrogate Models in Synthesis of Microwave Bandpass Filters," *EUROCON 2007 - The International Conference on "Computer as a Tool"*, 2007, pp. 98-101.

[50] F. Feng, C. Zhang, V. -M. -R. Gongal-Reddy, and Q. -J. Zhang, "Knowledge-based coarse and fine mesh space mapping approach to EM optimization," *2014 International Conference on Numerical Electromagnetic Modeling and Optimization for RF, Microwave, and Terahertz Applications (NEMO)*, 2014, pp. 1-4.

[51] B. Liu, H. Yang, and M. J. Lancaster, "Global Optimization of Microwave Filters Based on a Surrogate Model-Assisted Evolutionary Algorithm," *IEEE Trans. Microw. Theory Techn.*, vol. 65, no. 6, pp. 1976-1985, Jun. 2017.

[52] B. Gustavsen and A. Semlyen, "Rational approximation of frequency domain responses by vector fitting," *IEEE Trans. Power Deliv.*, vol. 14, no. 3, pp. 1052-1061, Jul. 1999.

[53] S. Koziel, X. S. Yang, and Q. J. Zhang, *Simulation-driven Design Optimization and Modeling for Microwave Engineering*. London, U.K.: Imperial College Press, 2013.

[54] D. C. Montgomery, *Design and analysis of experiments*. John wiley & sons, 2017.

[55] N. Metropolis and S. Ulam, "The Monte Carlo method," *Journal of the American Statal Association*, vol. 44, no. 247, pp. 335-341, Sep. 1949.

[56] M.D. Mckay, R.J. Beckman, and W.J. Conover, "A comparison of three methods for selecting values of input variables in the analysis of output from a computer code," *Technometrics*, vol. 21, no. 2, pp. 239 -245, 1979.

[57] Z. Zhang, H. C. Chen and Q. S. Cheng, "Surrogate-Assisted Quasi-Newton Enhanced Global Optimization of Antennas Based on a Heuristic Hypersphere Sampling," *IEEE Trans. Antennas Propag.*, vol. 69, no. 5, pp. 2993-2998, May 2021.

[58] Z. Zhang, Q. S. Cheng, H. Chen and F. Jiang, "An efficient hybrid sampling method for neural network-based microwave component modeling and optimization," *IEEE Microw. and Wirel. Compon. Letters*, vol. 30, no. 7, pp. 625-628, July 2020.

[59] W. Na and Q. Zhang, "Automated parametric modeling of microwave components using combined neural network and interpolation techniques," *2013 IEEE MTT-S International Microwave Symposium Digest (IMS)*, Seattle, WA, 2014, pp. 1-3.

[60] W. Na, K. Liu, H. Cai, W. Zhang, H. Xie, and D. Jin, "Efficient EM Optimization Exploiting Parallel Local Sampling Strategy and Bayesian Optimization for Microwave Applications," *IEEE Microw. Wirel. Compon. Lett.*, vol. 31, no. 10, pp. 1103-1106, Oct. 2021.

[61] W. Zhang, F. Feng, S. Yan, W. Na, J. Ma, and Q. Zhang, "EM-Centric Multiphysics Optimization of Microwave Components Using Parallel Computational Approach," *IEEE Trans. Microw. Theory Techn.*, vol. 68, no. 2, pp. 479-489, Feb. 2020.

[62] Y. Song, Q. S. Cheng, and S. Koziel, "Multi-fidelity local surrogate model for computationally efficient microwave component design optimization," *Sensors*, vol. 19, no. 13, Jul., 2019.

[63] J. Zhou, B. Duan, and J. Huang, "Influence and tuning of tunable screws for microwave filters using least squares support vector regression," *Int. J. RF and Microwave Comp. Aid. Eng.*, 20: 422-429, 2010.

[64] M. Sedaghat, R. Trinchero, and F. Canavero, "Compressed Machine Learning-Based Inverse Model for the Design of Microwave Filters," *2021 IEEE MTT-S International Microwave Symposium (IMS)*, 2021, pp. 13-15.

[65] F. Feng, W. Na, J. Jin, W. Zhang, and Q. -J. Zhang, "ANNs for Fast Parameterized EM Modeling: The State of the Art in Machine Learning for Design Automation of Passive Microwave Structures," *IEEE Microw. Mag.*, vol. 22, no. 10, pp. 37-50, Oct. 2021.

[66] V. K. Devabhaktuni, M. C. E. Yagoub, and Q. J. Zhang, "A robust algorithm for automatic development of neural network models for microwave applications," *IEEE Trans. Microw. Theory Techn.*, vol. 49, no. 12, pp. 2282–2291, Dec. 2001.

[67] H. Kabir, Y. Wang, M. Yu and Q. Zhang, "Neural Network Inverse Modeling and Applications to Microwave Filter Design," *IEEE Trans. Microw. Theory Techn.*, vol.56, no.4, pp: 867-879, 2008

[68] C. Zhang, J. Jin, W. C. Na, et al. "Multivalued Neural Network Inverse Modeling and Applications to Microwave Filters", *IEEE Trans. Microw. Theory Techn.*, vol. 66, no.8, pp:3781-3797, 2018.

[69] V. K. Devabhaktuni, B. Chattaraj, M. C. E. Yagoub, and Q.-J. Zhang, "Advanced microwave modeling framework exploiting automatic model generation, knowledge neural networks, and space mapping," *IEEE Trans. Microw. Theory Techn.*, vol. 51, no. 7, pp. 1822–1833, Jul. 2003.

[70] W. Na and Q.-J. Zhang, "Automated knowledge-based neural network modeling for microwave applications," *IEEE Microw. Wireless Compon. Lett.*, vol. 24, no. 7, pp. 499–501, Jul. 2014.

[71] J. Zhang, F. Feng, J. Jin, W. Zhang, Z. Zhao, and Q. -J. Zhang, "Adaptively Weighted Yield-Driven EM Optimization Incorporating Neuro-transfer Function Surrogate With Applications to Microwave Filters," *IEEE Trans. Microw. Theory Techn.*, vol. 69, no.1, pp: 518-528, 2021.

[72] J. Zhang, F. Feng, and Q. -J. Zhang, "Rapid Yield Estimation of Microwave Passive Components Using Model-Order Reduction Based Neuro-Transfer Function Models," *IEEE Microw. Wirel. Compon. Lett.*, vol. 31, no.4, pp: 333-336, 2021.

[73] W. Zhang et al., "Space mapping approach to electromagnetic centric multiphysics parametric modeling of microwave components," *IEEE Trans. Microw. Theory Techn.*, vol. 66, no. 7, pp. 169–3185, Jul. 2018.

[74] W. Zhang, F. Feng, J. Zhang, S. Zhang, V. M. R. Gongal-Reddy, and Q. J. Zhang, "Advanced parametric modeling using neuro-transfer function for EM based multiphysics analysis of microwave passive components," *in IEEE MTT-S Int. Microw. Symp. Dig.*, San Francisco, CA, USA, May 2016, pp. 1–3.

[75] W. Zhang et al., "Advanced Parallel Space-Mapping-Based Multiphysics Optimization for High-Power Microwave Filters," *IEEE Trans. Microw. Theory Techn.*, vol. 69, no. 5, pp. 2470-2484, May 2021.

[76] J. Dalton and A. Deshmane, "Artificial neural networks," IEEE Potentials, vol. 10, no. 2, pp. 33–36, 1991.

[77] L. -Y. Xiao, W. Shao, X. Ding and B. -Z. Wang, "Dynamic Adjustment Kernel Extreme Learning Machine for Microwave Component Design," *IEEE Trans. Microw. Theory Techn.*, vol. 66, no. 10, pp. 4452-4461, Oct. 2018.

[78] L. Xiao, W. Shao, F. Jin, B. Wang, W. T. Joines, and Q. H. Liu, "Semisupervised radial basis function neural network with an effective sampling strategy," *IEEE Trans. Microw. Theory Techn.*, vol. 68, no. 4, pp. 1260–1269, Apr. 2020.

[79] Z. Zhang, B. Liu, Y. Yang, Q. S. Cheng, "A Microwave Filter Yield Optimization Method Based on Offline Surrogate Model Assisted

Evolutionary Algorithm," *IEEE Trans. Microw. Theory Techn.*, doi: 10.1109/TMTT.2022.3163745.
[80] J. Jin, C. Zhang, F. Feng, W. Na, J. Ma, and Q. J. Zhang, "Deep neural network technique for high-dimensional microwave modeling and applications to parameter extraction of microwave filters," *IEEE Trans. Microw. Theory Techn.*, vol. 67, no. 10, pp. 4140–4155, Oct. 2019.
[81] S. Theodoridis and M. Mavroforakis, "Reduced convex hulls: A geometric approach to support vector machines," *IEEE Signal Process. Mag.*, vol. 24, no. 3, pp. 119–122, 2007.
[82] W.-H. Cao, C. Liu, Y. Yuan, M. Wu, S.-B. Wu, "Parametric modeling of microwave filter using combined MLS-SVR and pole-residue-based transfer functions," *Int. J. RF Microw. Comput. Aided Eng*. vol. 28, pp: e21246, 2018.
[83] J. Zhou and J. Huang, "Support-vector modeling and optimization for microwave filters manufacturing using small data sets," *IEEE 10th International Conference on Industrial Informatics*, 2012, pp. 202-207.
[84] Y. Yu, B. Liu, Y. Wang, and Q. S. Cheng, "Automated Diplexer Design With Key Performance Indicator-Based Objectives," in IEEE Microwave and Wireless Components Letters, doi: 10.1109/LMWC.2022.3150312.
[85] G. Zhang, H. He, and, and D. Katabi, "Circuit-GNN: Graph neural networks for distributed circuit design," *in Proc. 36th Int. Conf. Mach. Learning*, June 2019, vol. 97, pp. 7364–7373.
[86] G. Pan, Y. Wu, M. Yu, L. Fu, and H. Li, "Inverse Modeling for Filters Using a Regularized Deep Neural Network Approach," *IEEE Microw. Wirel. Compon. Lett.*, vol. 30, no. 5, pp. 457-460, May 2020.
[87] J. Liu and K. -L. Wu, "Filter Model Extraction with Convolutional Neural Network Based on Magnitude Information," *2021 IEEE MTT-S International Microwave Filter Workshop (IMFW)*, 2021, pp. 43-45.
[88] J.-J. Sun, S. Sun, X. Yu, Y. P. Chen, and J. Hu, "A deep neural network based tuning technique of lossy microwave coupled resonator filters," *Microw. Opt. Technol. Lett.*, vol. 61, pp: 2169– 2173, 2019.
[89] S. Koziel and J.W. Bandler. "Rapid Yield Estimation and Optimization of Microwave Structures Exploiting Feature-Based Statistical Analysis", *IEEE Trans. Microw. Theory Techn*, 2015, 63(1): 107 - 114.
[90] S. Koziel and J.W. Bandler, "Reliable microwave modeling by means of variable-fidelity response features," *IEEE Trans. Microw. Theory Techn.*, vol. 63, no. 12, pp. 4247-4254, Nov. 2015.
[91] N. Leszczynska, L. Szydlowski, and M. Mrozowski, "Zero-pole space mapping for CAD of filters," *IEEE Microw. Wirel. Compon. Lett.*, vol. 24, no. 9, pp. 581-583, Jul. 2014.
[92] C. Zhang, F. Feng, V. M. R. Gongal-Reddy, Q. J. Zhang, and J. W. Bandler, "Cognition-driven formulation of space mapping for equalripple optimization of microwave filters," *IEEE Trans. Microw. Theory Techn.*, vol. 63, no. 7, pp. 2154-2165, Jul. 2015.
[93] F. Feng, W. Na, W. Liu, S. Yan, L. Zhu, J. Ma, and Q. J. Zhang, "Multifeature assisted neuro-transfer function surrogate-based EM optimization exploiting trust region algorithms for microwave filter design," *IEEE Trans. Microw. Theory Techn.*, vol. 68, no. 2, pp. 531-542, Feb. 2020.
[94] F. Feng, C. Zhang, S. Zhang, V. M. R. Gongal-Reddy, and Q. J. Zhang, "Parallel EM optimization approach to microwave filter design using feature assisted neuro-transfer functions," *in IEEE MTT-S Int. Microw. Symp. Dig.*, San Francisco, CA, May. 2016, pp. 1-3.
[95] S. Koziel, L. Leifsson, I. Couckuyt, and T. Dhaene, "Robust variable-fidelity optimization of microwave filters using co-Kriging and trust regions," *Microw. Opt. Technol. Lett.*, vol. 55, pp: 765-769, 2013.
[96] J. E. Rayas-Sanchez and V. Gutierrez-Ayala, "Em-based monte carlo analysis and yield prediction of microwave circuits using linear-input neural-output space mapping," IEEE Transactions on Microwave Theory and Techniques, vol. 54, no. 12, pp. 4528–4537, 2006.
[97] W. Zhang, F. Feng, J. Jin and Q. -J. Zhang, "Parallel Multiphysics Optimization for Microwave Devices Exploiting Neural Network Surrogate," in IEEE Microwave and Wireless Components Letters, vol. 31, no. 4, pp. 341-344, April 2021.
[98] J. Zhang, F. Feng, J. Jin, W. Zhang, and Q. J. Zhang, "Adaptively weighted yield-driven em optimization incorporating neurotransfer function surrogate with applications to microwave filters," *IEEE Trans. Microw. Theory Techn.*, vol. 69, no. 1, pp. 518–528, 2021.
[99] S. Koziel and A. Bekasiewicz, "Rapid design optimization of microwave filters using variable-fidelity EM simulations and adjoint sensitivity," *2015 European Microwave Conference (EuMC)*, 2015, pp. 956-959.
[100] S. Li, X. Fan, P. D. Laforge, and Q. S. Cheng, "Surrogate Model-Based Space Mapping in Postfabrication Bandpass Filters' Tuning," *IEEE Trans. Microw. Theory Techn*, vol. 68, no. 6, pp. 2172-2182, June 2020.
[101] P. Zhao and K. Wu, "Homotopy Optimization of Microwave and Millimeter-Wave Filters Based on Neural Network Model," *IEEE Trans. Microw. Theory Techn.*, vol. 68, no. 4, pp. 1390-1400, April 2020.
[102] P. -W. Shu, Q. -X. Chu and J. -Y. Mai, "Harris Hawks Optimization Algorithm for Waveguide Filter Designs," *2020 IEEE Asia-Pacific Microwave Conference (APMC)*, 2020, pp. 406-408.
[103] Y. Jiao, Z. Zhang, Y. Yu and Q. S. Cheng, "Feature-based Surrogate-assisted Harris Hawks Optimization Algorithm for Microwave Filters," *2021 International Applied Computational Electromagnetics Society (ACES-China) Symposium*, 2021, pp. 1-2.
[104] D. Ninković and D. Olćan, "Genetic Algorithm Applied to Discrete Optimization of Band-Pass Microwave Filter," *2020 28th Telecommunications Forum (TELFOR)*, 2020, pp. 1-4.
[105] Y. Wang, Z. Zhang, Y. Yi, Y. Zhang, "Accurate microwave filter design based on particle swarm optimization and one-dimensional convolution autoencoders," *Int J RF Microw Comput Aided Eng.*, pp; e23034, 2021.
[106] C. Bachiller, H. Esteban, V. E. Boria, J. V. Morro, M. Taroncher and B. Gimeno, "CAD of evanescent mode waveguide filters with circular dielectric resonators," *2006 IEEE Antennas and Propagation Society International Symposium*, 2006, pp. 1567-1570.
[107] M. Yahia, R. Thabet, J. Tao, and M. L. Riabi, "Ridged waveguide filter optimization using an improved simplex method," *2012 6th International Conference on Sciences of Electronics, Technologies of Information and Telecommunications (SETIT)*, 2012, pp. 203-206.
[108] C. Erredir, M. L. Riabi, H. Ammari, and E. Bouarroudj, "Modeling of microwave filters using gradient Particle Swarm Optimization neural networks," *2017 Seminar on Detection Systems Architectures and Technologies (DAT)*, 2017, pp. 1-5.
[109] G. D'Antona, A. Monti, F. Ponci, and L. Rocca, "Maximum Entropy Analytical Solution for Stochastic Differential Equations Based on the Wiener-Askey Polynomial Chaos," *Proceedings of the 2006 IEEE International Workshop on Advanced Methods for Uncertainty Estimation in Measurement (AMUEM 2006)*, 2006, pp. 62-66, doi: 10.1109/AMYEM.2006.1650751.
[110] J. Zhang, F. Feng, W. Na, S. Yan, and Q. Zhang, "Parallel space-mapping based yield-driven em optimization incorporating trust region algorithm and polynomial chaos expansion," *IEEE Access*, vol. 7, pp. 143 673–143 683, 2019.
[111] J. Zhang, C. Zhang, F. Feng, W. Zhang, J. Ma, and Q. J. Zhang, "Polynomial chaos-based approach to yield-driven EM optimization," *IEEE Trans. Microw. Theory Techn.*, pp. 3186– 3199, 2018.
[112] Z. Zhang, H. Chen, Y. Yu, F. Jiang, and Q. S. Cheng, "Yield-constrained optimization design using polynomial chaos for microwave filters," *IEEE Access*, vol. 9, pp. 22 408–22 416.
[113] M. Baranowski, Ł. Balewski, A. Lamecki, and M. Mrozowski, "Design of Cavity Resonators Applying Shape Deformation Techniques," *2021 IEEE MTT-S International Microwave Filter Workshop (IMFW)*, 2021, pp. 291-293.
[114] M. Baranowski, Ł. Balewski, A. Lamecki, M. Mrozowski, and J. Galdeano, "The Design of Cavity Resonators and Microwave Filters Applying Shape Deformation Techniques," [Online], Available: https://www.techrxiv.org/articles/preprint/The_Design_of_Cavity_Resonators_and_Microwave_Filters_Applying_Shape_Deformation_Techniques/19114457.
[115] J. Jin, F. Feng, J. Zhang, J. Ma and Q. -J. Zhang, "Efficient EM Topology Optimization Incorporating Advanced Matrix Padé Via Lanczos and Genetic Algorithm for Microwave Design," *IEEE Trans. Microw. Theory Techn.*, vol. 69, no. 8, pp. 3645-3666, Aug. 2021.
[116] J. Zhang, F. Feng, W. Zhang, J. Jin, J. Ma and Q. Zhang, "A Novel Training Approach for Parametric Modeling of Microwave Passive Components Using Padé via Lanczos and EM Sensitivities," *IEEE Trans. Microw. Theory Techn.*, vol. 68, no. 6, pp. 2215-2233, June 2020.
[117] C. X. Mao, Y. Zhang, X. Y. Zhang, P. Xiao, Y. Wang and S. Gao, "Filtering Antennas: Design Methods and Recent Developments," *IEEE Microw. Mag.*, vol. 22, no. 11, pp. 52-63, Nov. 2021.
[118] Y. Gao et al., "Substrate Integrated Waveguide Filter–Amplifier Design Using Active Coupling Matrix Technique," *IEEE Trans. Microw. Theory Techn.*, vol. 68, no. 5, pp. 1706-1716, May 2020.
[119] Y. Gao, J. Powell, X. Shang, and M. J. Lancaster, "Coupling Matrix-Based Design of Waveguide Filter Amplifiers," *IEEE Trans. Microw. Theory Techn.*, vol. 66, no. 12, pp. 5300-5309, Dec. 2018.